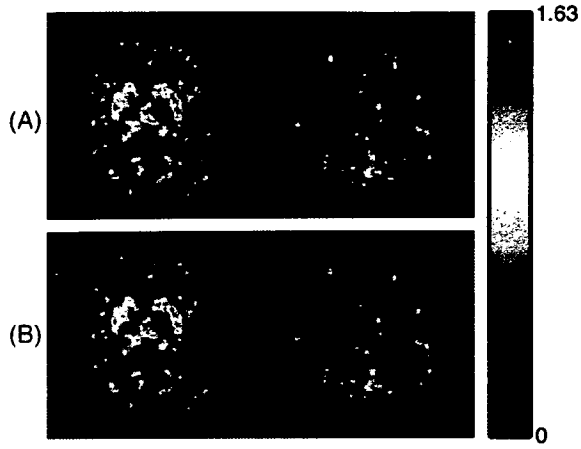

Fig. 7. Example of the parametric images of the BP_{ND} in [^{11}C]TMSX PET data using the robust EPISA-estimated intpTAC (A) and the measured intpTAC with metabolite correction (B). These images were calculated from the V_T images and a reference region.

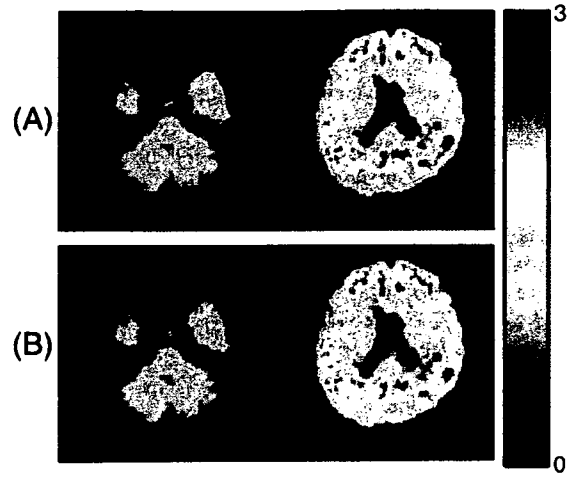

Fig. 9. Example of the parametric images of [^{11}C]PIB DVR in brain with Alzheimer disease. These images were calculated from the V_T images and a reference region using the robust EPISA-estimated intpTAC (A) and the measured intpTAC with metabolite correction (B).

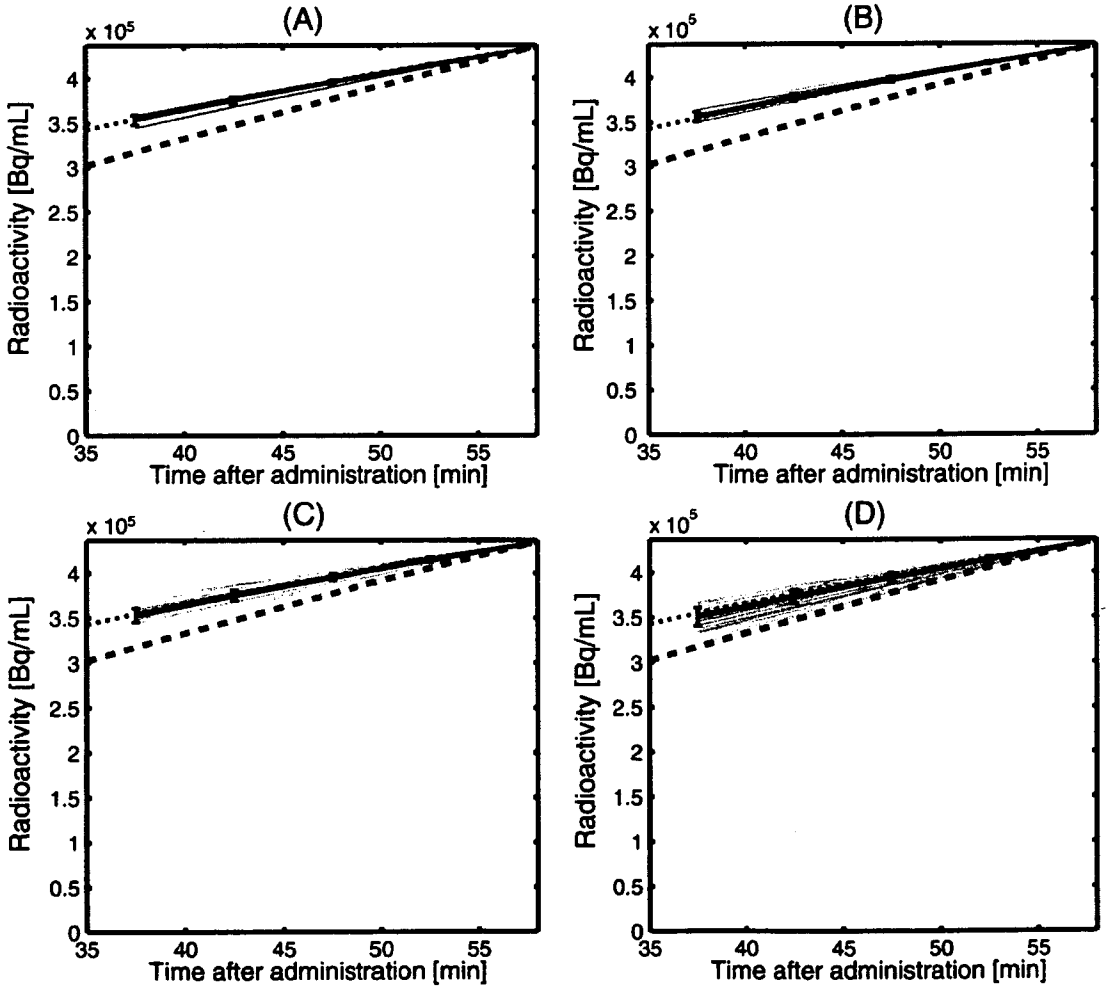

Fig. 8. Typical example of robust EPISA-estimated intpTACs (black solid line) in [^{11}C]PIB. The number of clusters was set to (A) 10, (B) 20, (C) 40, and (D) 80. Measured intpTACs with and without metabolite correction were plotted in black dotted line and gray break line. Standard deviation was calculated from the candidate intpTACs that were shown in gray solid lines.

Compartmental analysis of [^{11}C]flumazenil kinetics for the estimation of ligand transport rate and receptor distribution using positron emission tomography. J. Cereb. Blood Flow Metab. 11 (5), 735–744.

Lammertsma, A.A., Hume, S.P., 1996. Simplified reference tissue model for PET receptor studies. NeuroImage 4, 153–158.

Lee, J.S., Lee, D.S., Ahn, J.Y., Cheon, G.J., Kim, S.K., Yeo, J.S., Seo, K., Park, K.S., Chung, J.K., Lee, M.C., 2001. Blind separation of cardiac components and extraction of input function from $H_2{}^{15}O$ dynamic myocardial PET using independent component analysis. J. Nucl. Med. 42 (6), 938–943.

Logan, J., Fowler, J.S., Volkow, N.D., Wolf, A.P., Dewey, A.L., Schlyer, D.J., MacGregor, R.R., Hitzeman, R., Bendriem, B., Gatley, S.J., Christman, D.R., 1990. Graphical analysis of reversible radioligand binding from time–activity measurements applied to [*n*-^{11}C-methyl]-(−)-cocaine PET studies in human subjects. J. Cereb. Blood Flow Metab. 10 (5), 740–747.

Logan, J., Fowler, J.S., Volkow, N.D., Wang, G.-J., Ding, Y.-S., Alexoff, D.L., 1996. Distribution volume ratios without blood sampling from graphical analysis of PET data. J. Cereb. Blood Flow Metab. 16 (5), 834–840.

Lopresti, B.J., Klunk, W.E., Mathis, C.A., Hoge, J.A., Ziolko, S.K., Lu, X., Meltzer, C.C., Schimmerl, K., Tsopelas, N.D., DeKosky, S.T., Price, J.C., 2005. Simplified quantification of Pittsburgh Compound B amyloid imaging PET studies: a comparative analysis. J. Nucl. Med. 46 (12), 1959–1972.

Mathis, C.A., Wang, Y., Holt, D.P., Huang, G.-F., Debnath, M.L., Klunk, W.E., 2003. Synthesis and evaluation of ^{11}C-labeled 6-substituted 2-arylbenzothiazoles as amyloid imaging agents. J. Med. Chem. 46 (13), 2740–2754.

Mishina, M., Ishiwata, K., Kimura, Y., Naganawa, M., Oda, K., Kobayashi, S., Katayama, Y., Ishii, K., 2007. Evaluation of distribution of adenosine A_{2A} receptors in normal human brain measured with [^{11}C]TMSX PET. Synapse 61 (9), 778–784.

Naganawa, M., Kimura, Y., Ishii, K., Oda, K., Ishiwata, K., Matani, A., 2005a. Extraction of a plasma time–activity curve from dynamic brain PET images based on independent component analysis. IEEE Trans. Biomed. Eng. 52 (2), 201–210.

Naganawa, M., Kimura, Y., Nariai, T., Ishii, K., Oda, K., Manabe, Y., Chihara, K., Ishiwata, K., 2005b. Omission of serial arterial blood sampling in neuroreceptor imaging with independent component analysis. NeuroImage 26 (3), 885–890.

Naganawa, M., Kimura, Y., Ishii, K., Oda, K., Ishiwata, K., 2007a. Temporal and spatial blood information estimation using Bayesian ICA in dynamic cerebral positron emission tomography. Digit. Signal Process. 17 (5), 979–993.

Naganawa, M., Kimura, Y., Mishina, M., Manabe, Y., Chihara, K., Oda, K., Ishii, K., Ishiwata, K., 2007b. Quantification of adenosine A_{2A} receptors in the human brain using [^{11}C]TMSX and positron emission tomography. Eur. J. Nucl. Med. Mol. Imaging 34 (5), 679–687.

Di Paola, R., Bazin, J.P., Aubry, F., Aurengo, A., Cavailloles, F., Herry, J.Y., Kahn, E., 1982. Handling of dynamic sequences in nuclear medicine. IEEE Trans. Nucl. Sci. NS-29 (4), 1310–1321.

Price, J.C., Klunk, W.E., Lopresti, B.J., Lu, X., Hoge, J.A., Ziolko, S.K., Holt, D.P., Meltzer, C.C., DeKosky, S.T., Mathis, C.A., 2005. Kinetic modeling of amyloid binding in humans using PET imaging and Pittsburgh Compound-B. J. Cereb. Blood Flow Metab. 25 (11), 1528–1547.

Wang, Z.J., Peng, Q., Liu, K.J.R., Szabo, Z., 2005. Model-based receptor quantization analysis for PET parametric imaging. 27th Annual International Conference of the IEEE Engineering in Medicine and Biology Society, pp. 5908–5911.

Watabe, H., Channing, M.A., Der, M.G., Adams, H.R., Jagoda, E., Herscovitch, P., Eckelman, W.C., Carson, R.E., 2000. Kinetic analysis of the 5-HT_{2A} ligand [^{11}C]MDL 100,907. J. Cereb. Blood Flow Metab. 20, 899–909.

Wu, H.M., Hoh, C.K., Choi, Y., Schelbert, H.R., Hawkins, R.A., Phelps, M.E., Huang, S.C., 1995. Factor analysis for extraction of blood time–activity curves in dynamic FDG-PET studies. J. Nucl. Med. 36 (9), 1714–1722.

Presynaptic and postsynaptic nigrostriatal dopaminergic functions in multiple system atrophy

Masaya Hashimoto[a,c], Keiichi Kawasaki[a], Masahiko Suzuki[a,c], Kazuko Mitani[a,d], Shigeo Murayama[b], Masahiro Mishina[a,e], Keiichi Oda[a], Yuichi Kimura[a], Kiichi Ishiwata[a], Kenji Ishii[a] and Kiyoharu Inoue[c]

[a]Positron Medical Center, [b]Department of Neuropathology, Tokyo Metropolitan Institute of Gerontology, [c]Department of Neurology, Jikei University School of Medicine, [d]Department of Neurology, Tokyo Metropolitan Geriatric Hospital, Tokyo and [e]Neurological Institute, Nippon Medical School Chiba Hokusoh Hospital, Chiba, Japan

Correspondence to Kenji Ishii, Positron Medical Center, Tokyo Metropolitan Institute of Gerontology, 1-1 Naka-cho, Itabashi-ku, Tokyo 173-0022, Japan
Tel: +81 3 3964 3241 EX3503; fax: +81 3 3964 2188; e-mail: ishii@pet.tmig.or.jp

Received 7 September 2007; accepted 30 October 2007

A simultaneous evaluation of presynaptic and postsynaptic dopaminergic positron emission tomography markers, the dopamine transporters and the dopamine D_2-like receptors, was performed in eight patients with parkinsonian phenotype of multiple system atrophy. Both presynaptic and postsynaptic markers were revealed to have declined in such a manner that they kept strong positive correlation throughout the striatum of all patients, suggesting that the degeneration process in the striatum may involve the entire structure of the dopaminergic synapse. In two L-3,4,dihydroxyphenyl-alanine-responsive cases, the balance of decline in two markers was relatively shifted to presynaptic dominant side. Correlative positron emission tomography study of presynaptic and postsynaptic dopaminergic function may be useful for the diagnosis of multiple system atrophy and to understand the mechanisms of its temporal L-3,4,dihydroxyphenyl-alanine responsiveness. *NeuroReport* 19:145–150 © 2008 Wolters Kluwer Health | Lippincott Williams & Wilkins.

Keywords: dopamine receptor, dopamine transporter, L-3,4,dihydroxyphenyl-alanine responsiveness, multiple system atrophy, Parkinson, positron emission tomography

Introduction

In patients with the parkinsonian phenotype of multiple system atrophy (MSA-P), a pathological abnormality is observed mainly in the substantia nigra (SN), striatum, ceruleus nucleus, pontine nuclei, inferior olivary nucleus, cerebellum, and spinal cord. The impairment is particularly severe in the SN and striatum [1], and neuronal loss and gliosis are the features of the pathology [2]. Neuroimaging studies using positron emission tomography (PET) [3] and single photon emission computed tomography techniques [4] have reported reduced glucose metabolism in the striatum and declined nigrostriatal dopaminergic neural transmission function in both the presynaptic and postsynaptic sites. No pathological or neuroimaging studies, however, have examined the relationship between the degeneration/dysfunction of nigrostriatal presynaptic and postsynaptic dopaminergic systems. It is well known that responses to L-3,4,dihydroxyphenyl-alanine (L-DOPA) are generally poor in MSA [1], and this is ascribable to the fact that the pathology of MSA involves not only SN but also the striatum where the dopamine receptors exist. A transient effect, however, is occasionally noted in the early stages in certain cases. Wenning *et al.* [5] proposed a hypothesis based on the pathological finding of a dissociation between the SN and striatal degeneration that may account for such L-DOPA responsiveness. No pathological or neuroimaging evidence that directly demonstrated the dissociation in such cases, however, has been found.

We simultaneously measured the presynaptic and postsynaptic nigrostriatal dopaminergic functions using PET in MSA-P patients, including L-DOPA-responsive cases, and the regional correlation of two parameters was analyzed in the striatum to examine the characteristics of the disease and the mechanisms of L-DOPA responsiveness.

Methods

This study was approved by the Ethical Committee of Tokyo Metropolitan Institute of Gerontology. The objective and effect of the PET examination on the human body were adequately explained to all participants, and written informed consent was obtained.

Participants

We studied eight patients (68.9±7.4 years old) clinically diagnosed as MSA-P according to the consensus criteria established by Gilman *et al.* [6] (Table 1). The MSA-P patients underwent PET examination following a 15-h deprivation of antiparkinsonian drugs. The primary symptom observed in all the patients was parkinsonism; further, during the course of the disease, parkinsonism was noted to be the cardinal symptom. Magnetic resonance imaging (MRI) examination was also performed. The characteristics of the patients are presented in Table 1. Among the eight cases of MSA-P, cases 1 and 2 apparently responded to L-DOPA at the time of the PET study, and the improvement

Table 1 Clinical features of the eight patients with the parkinsonian phenotype of multiple system atrophy

Patient no./age (years)/sex	Hoehn and Yahr stage	Disease duration (years)	Autonomic dysfunction	Cerebellar dysfunction	Pyramidal sign	MRI findings	L-DOPA response
1/79/Female	III	1	+	+	+	Put	+
2/73/Female	III	1	+	+	+	Put	+
3/66/Female	I	2	+	+	+	No findings	−
4/61/Female	IV	2	+	+	+	cbll/put	−
5/72/Male	V	3	+	−	+	Put	−
6/56/Male	IV	4	+	+	+	Pons/cbll/put	−
7/73/Female	III	6	+	+	+	Pons/cbll/put	−
8/71/Female	V	9	+	−	+	Put	−

Signal change in the pons/middle cerebellar peduncles includes pontine/cerebellar atrophy (pons/cbll); Slit-like signal change at the posterolateral putaminal margin includes putaminal atrophy (put). L-DOPA, L-3,4,dihydroxyphenyl-alanine.

in the symptoms of parkinsonism due to L-DOPA was confirmed by neurologists.

The healthy control group consisted of eight participants (five men and three women, 62.3 ± 6.9 years old) that did not have a past medical history of neurological and psychiatric disorders. They were diagnosed as normal after physical and neurological examinations, screening MRI scans, and Mini-Mental Scale Evaluation (>28). They had not taken any neuroleptic drugs and were not addicted to alcohol; no history of any other substance abuse was present.

Positron emission tomography scans

^{11}C-labeled 2β-carbomethoxy-3β-(4-fluorophenyl)-tropane ([^{11}C]CFT) as a marker of presynaptic dopaminergic function for dopamine transporters and ^{11}C-labeled raclopride ([^{11}C]RAC) as a marker of postsynaptic dopaminergic function for dopamine D_2-like receptors were used as tracers for PET [7,8]. The methods used for the preparation of the radiopharmaceuticals were as described previously [9,10].

All the participants underwent the two PET studies on the same day with a 3–4-h interval. PET images were acquired in three-dimensional mode using the SET-2400W (Shimadzu, Kyoto, Japan) scanner [11] at the Positron Medical Center, Tokyo Metropolitan Institute of Gerontology. The acquired PET images were 128 × 128 × 50 in matrix size with a 2 × 2 × 3.125-mm voxel size. In PET acquisition, 300 MBq each of [^{11}C]CFT and [^{11}C]RAC were administered by an intravenous bolus injection, and all participants rested in a supine position with their eyes open during the test. The specific activity and the amount of cold material injected were 5.4–47 MBq/nM and 1.2–8.6 nM, respectively, for [^{11}C]CFT and 10–130 MBq/nM and 0.42–3.1 nM, respectively, for [^{11}C]RAC. For three of the eight healthy control participants, a dynamic scan was performed for 90 min for the [^{11}C]CFT study in the morning and for 60 min for the [^{11}C]RAC study in the afternoon to estimate the binding potentials. To measure the uptakes of these two tracers, for the five healthy participants and all the patients, a static scan was performed 75–90 min after the injection of the [^{11}C]CFT and 40–55 min after the injection of [^{11}C]RAC, respectively. The attenuation was corrected by a transmission scan using a ^{68}Ga/^{68}Ge source.

Data analysis

The two PET images of the [^{11}C]CFT and [^{11}C]RAC examinations obtained from the same participant were coregistered using an automated image registration program [12]. The images were processed further using Dr View software (AJS, Tokyo, Japan) on Linux workstations. Next, the images were resliced in the transaxial direction parallel to the anterior–posterior intercommissural (AC-PC) line, and the regions of interest (ROIs) were placed on the three subregions of the striatum – the bilateral caudate nuclei, anterior putamen, and posterior putamen – in two slices, that is, the AC-PC plane and 3.1 mm above the AC-PC line. ROIs of the striatum consisted of circles of 8-mm diameter. On each side of each slice, we set one ROI in the caudate and two ROIs each in the anterior and posterior putamen. The reference regions of the occipital lobe were placed in four slices in a range of 12.5–21.9 mm above the AC-PC plane. The reference region of the occipital lobe consisted of circles of 10-mm diameter, and we set four such circles on each side of each slice.

First, for dynamic scan data, the binding potential of the tracer in the bilateral caudate nuclei, anterior putamen, and posterior putamen of three healthy participants was estimated by a simplified reference region model [13] using the occipital lobe as a reference. Second, for static imaging, the uptake ratio index (URI) was calculated for all participants by the following formula:

$$\mathrm{URI} = \left(\mathrm{Activity}_{\mathrm{Striatum\ subregion}} - \mathrm{Activity}_{\mathrm{Occipital\ lobe}}\right) / \mathrm{Activity}_{\mathrm{Occipital\ lobe}}$$

URI was also calculated for the dynamic scan in the three healthy control participants using the data obtained from an equivalent time-frame. The URI in each ROI was compared between MSA-P patients and control participants with the Mann–Whitney *U*-test with Bonferroni's correction for multiple comparisons.

Next, we examined the correlation between the binding potential and the URI.

Results

For each tracer, the URIs of the striatal subregions in the static image were linearly correlated with the binding potentials in the dynamic scan (r^2=0.92, P<0.0001 for [^{11}C]CFT and r^2=0.93, P<0.0001 for [^{11}C]RAC). Therefore, we adopt the URI in reference to the occipital cortex for the further analysis.

Figure 1 demonstrates the representative PET images of a normal participant and an MSA-P patient. In the MSA-P patient, the URIs of both [^{11}C]CFT and [^{11}C]RAC declined in the striatum compared with the normal participant (Fig. 1).

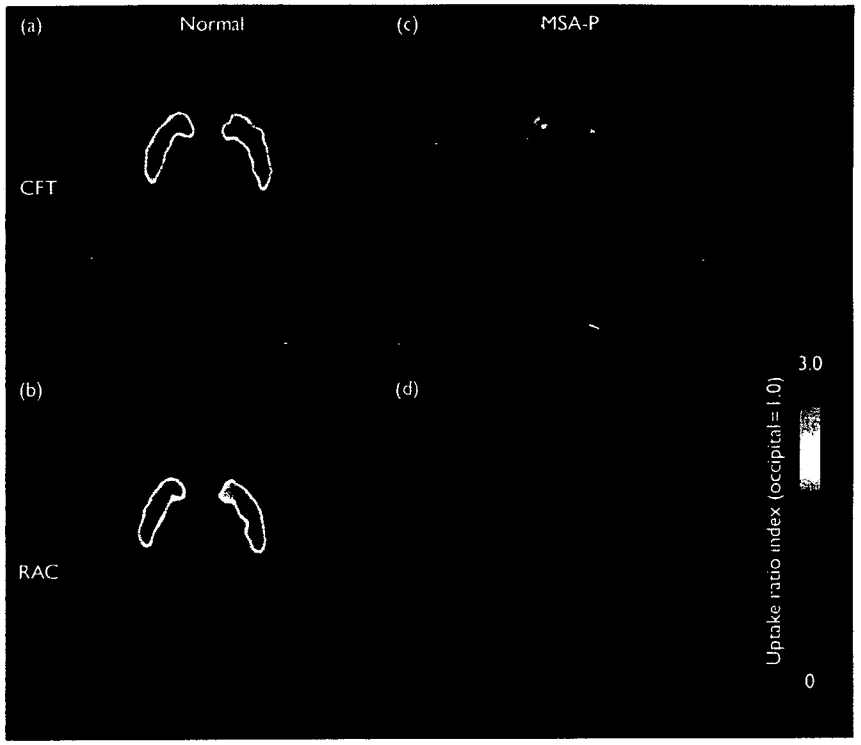

Fig. 1 Positron emission tomography images. (a) [^{11}C]CFT and (b) [^{11}C]RAC images were obtained from a normal participant, and (c) [^{11}C]CFT and (d) [^{11}C]RAC images were obtained from an MSA-P patient. All the images were normalized to the occipital lobe activity and obtained in a +3.1-mm plane from the anterior–posterior intercommissural line. [^{11}C]CFT, ^{11}C-labeled 2β-carbomethoxy-3β-(4-fluorophenyl)-tropane; [^{11}C]RAC, ^{11}C-labeled raclopride; MSA-P, phenotype of multiple system atrophy.

Table 2 The uptake ratio index of [^{11}C]CFT and [^{11}C]RAC in the subregions of the striatum

	Normal participants (n=8)	MSA-P patients (n=8)	Percentage of control
Caudate			
[^{11}C]CFT	3.70±0.55	2.49±0.41*	67.3
[^{11}C]RAC	3.46±0.40	2.63±0.31*	76.0
Anterior putamen			
[^{11}C]CFT	4.04±0.45	1.97±0.45*	48.8
[^{11}C]RAC	3.97±0.31	2.46±0.46*	62.0
Posterior putamen			
[^{11}C]CFT	3.82±0.47	1.58±0.42*	41.4
[^{11}C]RAC	3.90±0.32	2.07±0.67*	53.1

*P<0.05 as compared with normal controls (Mann–Whitney U-test with Bonferroni's multiple comparison correction).
[^{11}C]CFT, ^{11}C-labeled 2β-carbomethoxy-3β-(4-fluorophenyl)-tropane; [^{11}C]RAC, ^{11}C-labeled raclopride; MSA-P, phenotype of multiple system atrophy.

The results of ROI measurement are summarized in Table 2. In the MSA-P group, the URIs of both [^{11}C]CFT and [^{11}C]RAC significantly decreased in all the subdivisions of the striatum (P<0.05) in comparison with the control group, and the decrease was most prominent in the posterior putamen and relatively smaller in the caudate nuclei.

Scatter plots of the entire uptake data in individual participants for each of the three regions are shown in Fig. 2a–c and those for all areas are shown in Fig. 2d. A strong positive correlation was noted between the URIs of [^{11}C]CFT and [^{11}C]RAC in the MSA-P group. That is, the impairment of presynaptic and postsynaptic nigrostriatal dopaminergic function was observed in associative degree in all the subregions of the striatum.

Two patients apparently responded to the L-DOPA administration at the time of PET studies. Figure 2 indicates that the decrease in the [^{11}C]RAC uptake was relatively lesser in comparison with that in the [^{11}C]CFT uptake in the L-DOPA-responsive cases.

Discussion

In earlier studies, the cerebellum has been widely used as a reference region to estimate the availability of dopamine transporters using [^{11}C]CFT [14,15] and dopamine D_2-like receptors using [^{11}C]RAC [16]. We, however, selected the occipital cortex as a reference region in this study. Neuropharmacological evidence has revealed that the densities of both the dopamine transporters and dopamine D_2-like receptors in the human occipital cortex are negligible as in the case of the cerebellum [17]. Furthermore, the cerebellum is often involved in the pathological processes in MSA-P, whereas the occipital lobe is less likely to be affected. The selection of the occipital region as a reference would be useful for PET analysis of MSA. In contrast, the measured values of the striatum might have been affected by the atrophy. The correlation of two PET measures on the same regions, however, are robust because they are evaluated with common ROIs to cancel out the spatial effect.

Using [^{11}C]CFT and [^{11}C]RAC, we simultaneously measured presynaptic and postsynaptic nigrostriatal dopaminergic

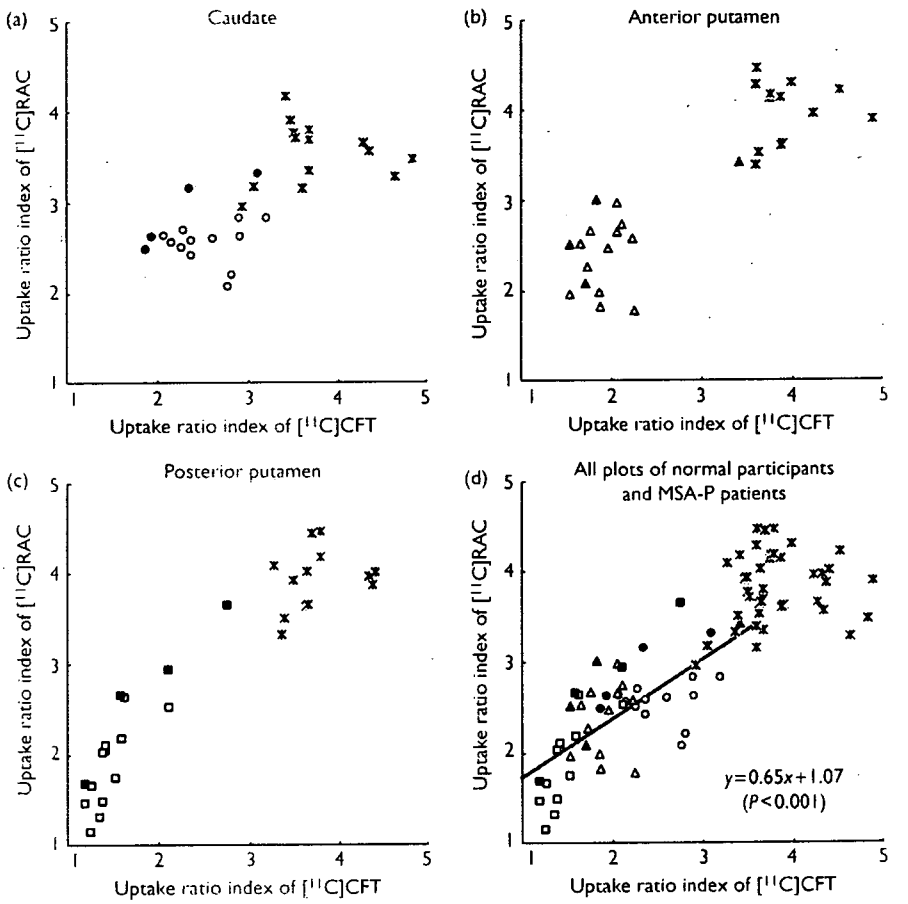

Fig. 2 The correlation between the uptake ratio index (URI) of [^{11}C]CFT and that of [^{11}C]RAC in the caudate nuclei (a), anterior putamen (b), posterior putamen (c), and all these areas (d) of all participants including MSA-P patients (n=8) and normal participants (n=8). The approximate lines for all the plots of the MSA-P group are shown in (d). Asterisk (*), normal participants; open circles (○), the caudate nuclei in MSA-P patients; open triangles (Δ), the anterior putamen in MSA-P patients; open squares (□), the posterior putamen in MSA-P patients; and solid markers (●), MSA-P patients exhibiting L-DOPA responsiveness. [^{11}C]CFT, ^{11}C-labeled 2β-carbomethoxy-3β-(4-fluorophenyl)-tropane; [^{11}C]RAC, ^{11}C-labeled raclopride; L-DOPA, L-3,4,dihydroxyphenyl-alanine; MSA-P, phenotype of multiple system atrophy.

functions and observed that both functions were significantly impaired in all eight patients with MSA-P compared with the normal group.

The functional impairment in the striatum was more noticeable in the putamen, particularly in its posterior part, than in the caudate nuclei. The most prominent result of our study was that a strong positive correlation was noted between presynaptic and postsynaptic functional impairments in the MSA-P group throughout the striatum regardless of the severity of the impairments. In Parkinson's disease (PD), presynaptic and postsynaptic functional impairments were reported to be negatively correlated in the putamen by PET using [^{11}C]CFT and [^{11}C]SCH 23390 (dopamine D_1-like receptor probe), reflecting severe impairment in the presynaptic marker with an upregulation of the postsynaptic function [18]. The differential diagnosis between MSA-P and PD in clinical situations is at times difficult. The patterns of presynaptic and postsynaptic functional impairments, however, demonstrated by PET contrasted between MSA-P and PD, and therefore the two disorders can be clearly differentiated with combined presynaptic and postsynaptic dopaminergic PET examinations.

Ghaemi *et al.* [3] applied PET using [^{18}F]FDOPA and [^{11}C]RAC to MSA-P patients and discovered that both presynaptic and postsynaptic dopaminergic functions were reduced in the nigrostriatal dopaminergic system. They did not, however, provide information about whether the impairments in the presynaptic and postsynaptic dopaminergic function were correlated in each patient. Our study is the first to demonstrate a positive correlation between the presynaptic and postsynaptic dopaminergic function with respect to the local subdivisions of the striatum and the disease duration.

What is the pathological background of the strong correlation of presynaptic and postsynaptic markers measured by PET? Pathologically, neuronal loss and gliosis are the primary forms of impairment in MSA [2]. The neuronal loss tends to be severe in both SN and striatum; however, it is not always to the same extent [1], and there has been no report regarding the correlation of pathological findings such as glial cytoplasmic inclusion [19] and α-synuclein [20,21] between SN and striatum. If the PET markers for presynaptic and postsynaptic dopaminergic function directly reflect the degree of degeneration in SN and striatum

independently, as in PD [15,22], the combination in the degree of presynaptic and postsynaptic functional impairment could be variable. The presence of a strong positive correlation between the presynaptic and postsynaptic dopaminergic functions measured by PET within patients and across patients suggests that these impairments in MSA-P are the result of the destruction of the entire synaptic structure in the striatum. Pathologically, the putamen is one of the areas with the most severe neuronal loss in MSA-P [2]. We consider that the presynaptic marker represents the degree of degeneration of the SN only if the striatum involvement is lesser than that of SN; however, once the severe destruction of striatum occurs, the presynaptic marker no longer represents the degree of SN degeneration because it is masked by the destruction of the entire structure of the synapse.

Parkinsonism in MSA is treated with L-DOPA, dopamine agonists, and anticholinergic agents; however, only a mild effect is noted in a minor population in the early stage, and the responsiveness to L-DOPA gradually disappears. Generally, responses to L-DOPA are poor in cases of MSA-P [1]. In a previous report, L-DOPA was effective in the early stage in approximately 1/3 of the MSA cases [23]. We examined two early MSA-P cases responsive to L-DOPA. In these cases, the presynaptic dopaminergic function was markedly reduced; however, the reduction in the postsynaptic dopaminergic function was relatively less severe compared with that in the cases not responsive to L-DOPA; moreover, this trend was more prominent in the striatum on the contralateral side in which L-DOPA alleviated the symptoms of parkinsonism. Churchyard *et al.* [24] suggested that the ineffectiveness of L-DOPA on parkinsonism in MSA is related to the dominance of neuronal loss, gliosis, and the reduction in postsynaptic dopamine D_2 receptors in the posterior putamen. Wenning *et al.* [5] reported that L-DOPA was highly effective in the cases in which the putamen was relatively conserved compared with the degree of nigral neuronal loss, and the effect of L-DOPA was negatively correlated with the degree of nigral degeneration, suggesting that nigral degeneration precedes striatal degeneration [1]. Whether nigral degeneration preceded striatal degeneration was not clear in our study; however, postsynaptic dopaminergic function was relatively retained in our L-DOPA-responsive cases. We consider that the degree of conservation of postsynaptic dopaminergic function is related to the effectiveness of L-DOPA in MSA-P and that a trend of dissociation of presynaptic and postsynaptic markers can be detected by PET. Further studies are necessary to increase the number of the participants and to follow up the L-DOPA-responsive cases using PET and clinical course observations.

Conclusion

We have established the presence of a strong positive correlation between the reductions in nigrostriatal presynaptic and postsynaptic dopaminergic functions and L-DOPA-responsive cases in which the degrees of presynaptic and postsynaptic functional impairments are dissociated in some manner.

The elucidation of the patterns and processes of presynaptic and postsynaptic functional impairments may provide a clue to understanding the development and advancement mechanisms of the disease and will aid in a more reliable early clinical diagnosis and prediction of drug effects.

References

1. Wenning GK, Ben-Shlomo Y, Magalhaes M, Daniel SE, Quinn NP. Clinicopathological study of 35 cases of multiple system atrophy. *J Neuro Neurosurg Psychiatry* 1995; 58:160–166.
2. James SL, Nigel L. Disorders of movement and system degeneration. In: David IG, Peter LL, editors. *Greenfield's Neuropathology.* 7th ed. Vol. 2. London: Arnold; 2002. pp. 325–430.
3. Ghaemi M, Hilker R, Rudolf J, Sobesky J, Heiss WD. Differentiating multiple system atrophy from Parkinson's disease: contribution of striatal and midbrain MRI volumetry and multi-tracer PET imaging. *J Neurol Neurosurg Psychiatry* 2002; 73:517–523.
4. Van Royen E, Verhoeff NF, Speelman JD, Wolters EC, Kuiper MA, Janssen AG. Multiple system atrophy and progressive supranuclear palsy. Diminished striatal D_2 dopamine receptor activity demonstrated by ^{123}I-IBZM single photon emission computed tomography. *Arch Neurol* 1993; 50:513–516.
5. Wenning GK, Quinn N, Magalhaes M, Mathias C, Daniel SE. 'Minimal change' multiple system atrophy. *Mov Disord* 1994; 9:161–166.
6. Gilman S, Low P, Quinn N, Albanese A, Ben-Shlomo Y, Fowler C, *et al.* Consensus statement on the diagnosis of multiple system atrophy. American Autonomic Society and American Academy of Neurology. *Clin Auton Res* 1998; 8:359–362.
7. Volkow ND, Fowler JS, Gatley SJ, Logan J, Wang GJ, Ding YS, *et al.* PET evaluation of the dopamine system of human brain. *J Nucl Med* 1996; 37:1242–1256.
8. Booij J, Tissingh G, Winogrodzka A, van Royen EA. Imaging of the dopaminergic neurotransmission system using single-photon emission tomography and positron emission tomography in patients with parkinsonism. *Eur J Nucl Med* 1999; 26:171–182.
9. Kawamura K, Oda K, Ishiwata K. Age-related changes of the [^{11}C]CFT binding to the striatal dopamine transporters in the Fischer 344 rats: a PET study. *Ann Nucl Med* 2003; 17:249–253.
10. Langer O, Någren K, Dolle F, Lundkvist C, Sandell J, Swahn CG, *et al.* Precursor synthesis and radiolabelling of the dopamine D_2 receptor ligand [^{11}C]raclopride from [^{11}C]methyl triflate. *J Labelled Comp Radiopharm* 1999; 42:1183–1193.
11. Fujiwara T, Watanuki S, Yamamoto S, Miyake M, Seo S, Itoh M, *et al.* Performance evaluation of a large axial field-of-view PET scanner: SET-2400W. *Ann Nucl Med* 1997; 11:307–313.
12. Ardekani BA, Braun M, Hutton BF, Kanno I, Iida H. A fully automatic multimodality image registration algorithm. *J Comput Assist Tomogr* 1995; 19:615–623.
13. Gunn RN, Lammertsma AA, Hume SP, Cunningham VJ. Parametric imaging of ligand-receptor binding in PET using a simplified reference region model. *NeuroImage* 1997; 6:279–287.
14. Wong DF, Yung B, Dannals RF, Shaya EK, Ravert HT, Chen CA, *et al.* In vivo imaging of baboon and human dopamine transporters by positron emission tomography using [^{11}C]WIN 35 428. *Synapse* 1993; 15:130–142.
15. Frost JJ, Rosier AJ, Reich SG, Smith JS, Ehlers MD, Snyder SH, *et al.* Positron emission tomographic imaging of the dopamine transporter with ^{11}C-WIN 35,428 reveals marked declines in mild Parkinson's disease. *Ann Neurol* 1993; 34:423–431.
16. Antonini A, Leenders KL, Reist H, Thomann R, Beer HF, Locher J. Effect of age on D_2 dopamine receptors in normal human brain measured by positron emission tomography and ^{11}C-raclopride. *Arch Neurol* 1993; 50:474–480.
17. Mozley PD, Stubbs JB, Kung HF, Selikson MH, Stabin MG, Alavi A. Biodistribution and dosimetry of iodine-123-IBF: a potent radiolig and for imaging the D2 dopamine receptor. *J Nucl Med* 1993; 34: 1910–1917.
18. Ouchi Y, Kanno T, Okada H, Yoshikawa E, Futatsubashi M, Nobezawa S, *et al.* Presynaptic and postsynaptic dopaminergic binding densities in the nigrostriatal and mesocortical systems in early Parkinson's disease: a double-tracer positron emission tomography study. *Ann Neurol* 1999; 46:723–731.
19. Papp MI, Kahn JE, Lantos PL. Glial cytoplasmic inclusions in the CNS of patients with multiple system atrophy (striatonigral degeneration,

olivopontocerebellar atrophy and Shy–Drager syndrome). *J Neurol Sci* 1989; 94:79–100.
20. Tu PH, Galvin JE, Baba M, Giasson B, Tomita T, Leight S, *et al.* Glial cytoplasmic inclusions in white matter oligodendrocytes of multiple system atrophy brains contain insoluble alpha-synuclein. *Ann Neurol* 1998; 44:415–422.
21. Wakabayashi K, Yoshimoto M, Tsuji S, Takahashi H. Alpha-synuclein immunoreactivity in glial cytoplasmic inclusions in multiple system atrophy. *Neurosci Lett* 1998; 249:180–182.
22. Snow BJ, Tooyama I, McGeer EG, Yamada T, Calne DB, Takahashi H, *et al.* Human positron emission tomographic [^{18}F]fluorodopa studies correlate with dopamine cell counts and levels. *Ann Neurol* 1993; 34:324–330.
23. Rajput AH, Rozdilsky B, Rajput A, Ang L. Levodopa efficacy and pathological basis of Parkinson syndrome. *Clin Neuropharmacol* 1990; 13:553–558.
24. Churchyard A, Donnan GA, Hughes A, Howells DW, Woodhouse D, Wong JY, *et al.* Dopa resistance in multiple-system atrophy: loss of postsynaptic D_2 receptors. *Ann Neurol* 1993; 34:219–226.

High Occupancy of Sigma-1 Receptors in the Human Brain after Single Oral Administration of Fluvoxamine: A Positron Emission Tomography Study Using [^{11}C]SA4503

Masatomo Ishikawa, Kiichi Ishiwata, Kenji Ishii, Yuichi Kimura, Muneyuki Sakata, Mika Naganawa, Keiichi Oda, Ryousuke Miyatake, Mihisa Fujisaki, Eiji Shimizu, Yukihiko Shirayama, Masaomi Iyo, and Kenji Hashimoto

Background: Sigma-1 receptors might be implicated in the pathophysiology of psychiatric diseases, as well as in the mechanisms of action of some selective serotonin reuptake inhibitors (SSRIs). Among the several SSRIs, fluvoxamine has the highest affinity for sigma-1 receptors (Ki = 36 nM), whereas paroxetine shows low affinity (Ki = 1893 nM). The present study was undertaken to examine whether fluvoxamine binds to sigma-1 receptors in living human brain.

Methods: A dynamic positron emission tomography (PET) data acquisition using the selective sigma-1 receptor ligand [^{11}C]SA4503 was performed with arterial blood sampling to evaluate quantitatively the binding of [^{11}C]SA4503 to sigma-1 receptors in 15 healthy male volunteers. Each subject had two PET scans before and after randomly receiving a single dose of either fluvoxamine (50, 100, 150, or 200 mg) or paroxetine (20 mg). The binding potential of [^{11}C]SA4503 in 9 regions of the brain was calculated by a 2-tissue 3-compartment model. In addition, we examined the effects of functional polymorphisms of the sigma-1 receptor (SIGMAR1) gene on the binding potential of [^{11}C]SA4503.

Results: Fluvoxamine bound to sigma-1 receptors in all brain regions in a dose-dependent manner, whereas paroxetine did not bind to sigma-1 receptors. However, there was no association between the SIGMAR1 gene polymorphism GC-241-240TT and binding potential.

Conclusions: The study demonstrated that fluvoxamine bound to sigma-1 receptors in living human brain at therapeutic doses. These findings suggest that sigma-1 receptors may play an important role in the mechanism of action of fluvoxamine.

Key Words: Fluvoxamine, occupancy, paroxetine, PET, sigma-1 receptor, SSRI

Selective serotonin reuptake inhibitors (SSRIs) have emerged as a major therapeutic advance in psychopharmacology. SSRIs are the treatment of choice for many indications, including major depressive disorder, dysthymia, obsessive-compulsive disorder, and obsessive-compulsive disorder spectrum disorders (which include panic disorder, eating disorders, and others), because of their efficacy, safety profile, tolerability, and low toxicity in case of overdose, as well as patient compliance (1,2). Although all the SSRIs share the blockade of the serotonin transporters that leads to elevation of serotonin levels throughout the central nervous system, it is well known that their pharmacology is quite heterogenous (3–11).

Sigma-1 receptors act as specific binding sites in the central nervous system, and they exert a potent modulation on a number of neurotransmitter systems, including the glutamatergic, noradrenergic, dopaminergic, serotonergic and cholinergic systems. Several lines of evidence suggest that sigma-1 receptors play a role in the pathophysiology of responses to stress and psychiatric diseases, including major depression, schizophrenia, cognition, and addiction (12–17). Cell biologically, sigma-1 receptors mainly reside on the endoplasmic reticulum and regulate Ca^{2+} signaling (18). Furthermore, sigma-1 receptors form a complex with the cytoskeletal adaptor protein ankyrin, and with stimulation to the sigma-1 receptor, it translocates to nuclear membranes and plasma membranes, suggesting that sigma-1 receptors have an important role in neuroplasticity (19). Narita *et al.* (3) reported that some SSRIs possess high to moderate affinities for sigma-1 receptors in rat brain. The rank order of affinity of SSRIs for sigma-1 receptors is as follows: fluvoxamine (Ki = 36 nM) > sertraline (Ki = 57 nM) > fluoxetine (Ki = 120 nM) > citalopram (Ki = 292 nM). In contrast, paroxetine (Ki = 1893 nM) has low affinity for sigma-1 receptors (3). Thus, it seems that sigma-1 receptors may play a role in the mechanism of action of some SSRIs, such as fluvoxamine (3,15,20).

Positron emission tomography (PET) is the most effective technique to estimate the receptor occupancy rates of drugs in human brain (21,22). Recently, it has been demonstrated that [^{11}C]SA4503 is a selective PET ligand for sigma-1 receptor in the brain (23–26). SA4503 has an affinity of approximately 17.4 nM (IC_{50}) for the sigma-1 receptor, which is about 100 times higher than those for sigma-2, α_1-adrenergic, dopamine D_2, serotonin $(5\text{-HT})_{1A}$, 5-HT_2, histamine H_1, muscarinic M_1, and muscarinic M_2 receptors, and has no affinity for other 29 receptors, ion channels, and second messenger systems (27). The inhibition curves of SA4503 for [^{3}H](+)pentazocine binding were shifted to the

From the Division of Clinical Neuroscience (MIs, KH), Chiba University Center for Forensic Mental Health; Graduate School of Information Science (MS), Nara Institute of Science and Technology; Japan Society for the Promotion of Science (MN); Department of Psychiatry (MIs, RM, MF, ES, YS, MIy), Chiba University Graduate School of Medicine, Chiba; Positron Medical Center (MIs, KI, KI, YK, MN, KO), Tokyo Metropolitan Institute of Gerontology, Tokyo, Japan.

Address reprint requests to Kenji Hashimoto, Ph.D., Division of Clinical Neuroscience, Chiba University Center for Forensic Mental Health, 1-8-1 Inohana, Chiba 260-8670, Japan; E-mail: hashimoto@faculty.chiba-u.jp.

Received February 7, 2007; revised March 31, 2007; accepted April 2, 2007.

0006-3223/07/$32.00
doi:10.1016/j.biopsych.2007.04.001

right in the presence of GTPγS, as similar to those of sigma-1 receptor agonists[(+)-3-PPP and (+)-pentazocine] (27). In addition, similar to sigma-1 receptor agonists [(+)-3-PPP and (+)-pentazocine], SA4503 significantly increased the Kd value, but not the Bmax value, for specific [^{3}H](+)pentazocine binding to sigma-1 receptors (27). These findings suggest that SA4503 is a sigma-1 receptor agonist (27). Binding of [^{11}C]SA4503 in the brains of patients with Alzheimer's or Parkinson's disease has been shown to be lower than in normal controls (15,28). Furthermore, Ishiwata *et al.* (29) reported a high occupancy of sigma-1 receptors (approximately 80%) as well as dopamine D_2 receptors (approximately 60%) in human brain after a single oral administration of the typical antipsychotic drug haloperidol (3 mg), suggesting that PET study using [^{11}C]SA4503 can be used for evaluating the sigma-1 receptor occupancy rates by therapeutic drugs in human brain (29).

The purpose of this study was to determine whether two SSRIs, fluvoxamine and paroxetine, bind to sigma-1 receptors in human brain by using [^{11}C]SA4503 and PET. In addition, we examined the effects of polymorphisms of the sigma-1 receptor (SIGMAR1; OMIM No. 601978) gene on the binding potential of [^{11}C]SA4503 in human brain, since polymorphisms (T-485A and GC-241-240TT; rs1799729) in the SIGMAR1 gene have been shown to be functional polymorphisms (30).

Methods and Materials

Subjects

This study was approved by the Ethical Committee of Tokyo Metropolitan Institute of Gerontology and the Ethics Committee of Chiba University Graduate School of Medicine. Fifteen healthy male volunteers participated in the study (mean age = 34.7 years, SD = 4.6, range = 28–41). Written informed consent was obtained from each subject after the procedures had been fully explained. None of the subjects had any neurological or psychological findings, or showed any abnormalities in the brain magnetic resonance imaging (MRI) scan taken between the two PET scans. None had been receiving any medications of any kind. None had a history of alcoholism.

[^{11}C]SA4503 and PET

Each volunteer participated in two [^{11}C]SA4503-PET scans, one before and one after oral administration of an SSRI. The SSRI was administered within 5 min after the end of the first PET scan. The second PET scan took place 4–4.5 hours after taking the SSRI to achieve an adequate level of drug concentration in blood. It has been reported that after oral administration of a single dose of fluvoxamine (50 mg) in healthy subjects, the concentration in blood reaches its peak in approximately 5–6 hours (31,32). Accordingly, we collected blood samples just before tracer injection of the second PET scan to monitor the concentration of fluvoxamine. The concentration of fluvoxamine in blood was measured by liquid chromatography followed by tandem mass spectrometry.

The volunteers were randomly administered either fluvoxamine (50, 100, 150 or 200 mg, n = 3; Luvox (Astellas Ltd, Tokyo, Japan) or paroxetine (20 mg, n = 3; Paxil (GlaxoSmithKline Ltd, Tokyo, Japan). All drug tablets were sealed in the same nondescript capsule so that both the volunteers and administrator would be blind to the contents. PET was performed at the Positron Medical Center, Tokyo Metropolitan Institute of Gerontology with a SET 2400W scanner (Shimadzu Co., Kyoto, Japan) (30,33). The spatial resolution was 4.4 mm full width at half maximum in the transverse direction and 6.5 mm full width at half maximum in the axial direction; the image matrix was 128 × 128 × 50 and the voxel size was 2 × 2 × 3.125 mm. [^{11}C]SA4503 was prepared as described previously (21,23). The injected doses of [^{11}C]SA4503 were 9.3 ± 2.1 MBq/.18 ± .16 nmol/kg (specific activity 79 ± 42 TBq/mmol). A transmission scan was performed with a rotating ^{68}Ga/^{68}Ge rod source for 5 min for attenuation correction before the administration of the tracer. A dynamic series of decay-corrected PET data acquisition was performed in the 2-dimensional mode for 90 min starting at the time of the intravenous bolus injection of [^{11}C]SA4503. The frame arrangement was 10 sec × 6 frames, 30 sec × 3 frames, 60 sec × 5 frames, 150 sec × 5 frames, and 300 sec × 14 frames. The dynamic image was reconstructed with a filtered back-projection algorithm using a Butterworth filter (1.25 cycles/cm, order 2).

Each subject was placed in a supine position with eyes closed. Immediately after the bolus injection, 12 arterial blood samples were collected at 10-sec intervals over 2 min, the next 2 samples were collected at 15-sec intervals over 30 sec, and the remaining 12 samples were collected at longer intervals, for a total of 26 samples. All samples were manually drawn. Plasma was separated, weighed and measured for radioactivity with a sodium iodide (Tl) well scintillation counter. Five samples collected at 3, 10, 20, 30, and 40 min were further processed by high performance liquid chromatography for metabolite analysis (23,34).

Data Analysis

Image manipulations were carried out on an O2 work station (Silicon Graphics Inc., Mountain View, California), using the medical image processing application package "Dr. View," version 5.2 (AJS Co. Ltd., Tokyo, Japan). Regions of interest were defined over the frontal, temporal, parietal, occipital, and anterior cingulate cortices, head of the caudate nucleus, putamen, thalamus, and cerebellum with reference to the coregistered MRI, which served as an anatomical guide.

Binding of [^{11}C]SA4503 to sigma-1 receptors was calculated as the binding potential by methods described elsewhere (34). Briefly, binding potentials were computed using a 2-tissue 3-compartment model (35). Sigma-1 receptor occupancy (%) by SSRI was calculated for each region of interest as 100' [(binding potential at baseline–binding potential at SSRI-loading)/binding potential at baseline]. Images of the distribution volumes of [^{11}C]SA4503 were calculated using the Logan plot method (34,36).

The relationship between sigma-1 receptor occupancy and the dose or blood concentration of fluvoxamine was modeled by the equation Occ = a (F/(F + ED50), where Occ refers to occupancy, F refers to dose or blood level of fluvoxamine, a is the maximal receptor occupancy and ED50 is the blood fluvoxamine level resulting in 50% maximal receptor occupancy.

Genotype Analysis

The genotypes of the T-485A and GC-241-240TT in the 5' untranslated region of the SIGMAR1 gene was analyzed in all volunteers according to methods previously described (30,37).

Statistical Analysis

The data are the mean ± SD. Statistical analysis was performed by using the software package SPSS (SPSS 12.0J; SPSS, Inc., Tokyo, Japan). The dose-dependent relationship was evaluated by one-way analysis of variance with contrast (polynomial). The relationship between the binding potential at baseline

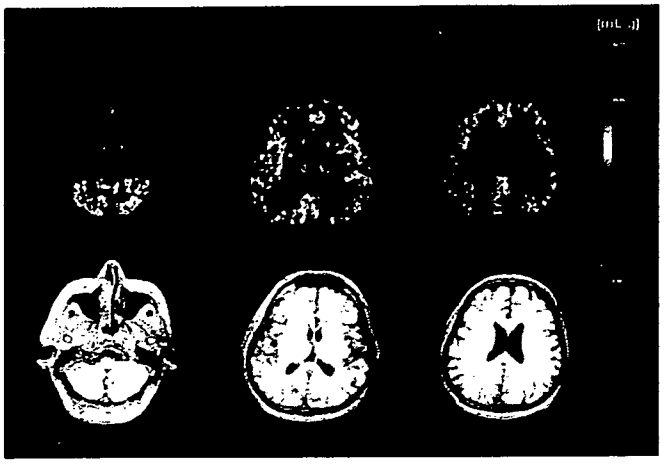

Figure 1. Representative images of the distribution volume of [^{11}C]SA4503-PET at baseline shown with corresponding MRI images. PET, positron emission tomography; MRI, magnetic resonance imaging.

and genotype of the SIGMAR1 gene was analyzed by one-way analysis of variance. Significance for the results was set at $p < .05$.

Results

Radioactivity was distributed throughout the human brain after intravenous administration of [^{11}C]SA4503. Representative parametric images of the distribution volume of [^{11}C]SA4503 at baseline are shown with corresponding MRI images in Figure 1. These results show that sigma-1 receptors are concentrated in brain areas of the limbic system, including areas involved in motor function, sensory perception, and endocrine function, consistent with the previous reports (29,34). Representative images of the distribution volume of [^{11}C]SA4503 in the fluvoxamine- and paroxetine-loading conditions are shown in Figure 2. A single administration of fluvoxamine (200 mg), but not paroxetine (20 mg), markedly decreased the distribution volume of [^{11}C]SA4503 (Figure 2). Table 1 shows the binding potentials and occupancy rates in 9 brain regions. [^{11}C]SA4503 bound throughout the brain, and the cerebellum showed the highest binding potential.

We analyzed whether the effects of fluvoxamine on occupancy of sigma-1 receptors were dose-dependent. Analysis using contrast (polynomial) showed that fluvoxamine significantly and dose-dependently bound to sigma-1 receptors in the frontal cortex ($p < .021$), parietal cortex ($p < .024$), occipital cortex ($p < .011$), head of the caudate nucleus ($p < .012$), thalamus ($p < .008$), and cerebellum ($p < .037$). The dose-dependency also seemed to be operative at the temporal cortex ($p < .069$), anterior cingulate gyrus ($p < .073$), and putamen ($p < .067$), but the correlation at these sites was not statistically significant. There were significant correlations between the blood concentration of fluvoxamine and occupancy in the brain regions (temporal cortex: $r = .62$, $p < .05$; parietal cortex: $r = .70$, $p < .05$; occipital cortex: $r = .63$, $p < .05$; head of the caudate nucleus: $r = .70$, $p < .05$; putamen: $r = .67$, $p < .05$; thalamus: $r = .62$, $p < .05$; cerebellum: $r = .77$, $p < .01$). There were weak correlations between the blood concentration of fluvoxamine and occupancy in the other two regions (frontal cortex; $r = .54$, $.05 < p < .1$; cingulate gyrus; $r = .564$, $.05 < p < .1$). Figure 3 shows representative data for the parietal cortex and cerebellum. There were statistically significant correlations between the sigma-1 receptor occupancy and dose or blood concentration of fluvoxamine in both these brain regions (Figure 3).

Next, we examined whether the SIGMAR1 gene polymorphisms affect the binding potential of sigma-1 receptors in human brain. However, all subjects showed TT genotype at the T-485A site. As for the GC-241-240TT polymorphism, 8 subjects had GC/GC genotype, and 5 subjects had GC/TT genotype, and 2 subjects had TT/TT genotype. There was no association between GC-241-240TT polymorphisms and the baseline binding potentials of sigma-1 receptors in any of the brain regions examined (Supplement 1).

Discussion

The major finding of this study is that, after a single oral administration, fluvoxamine bound to sigma-1 receptors in the living human brain in a dose-dependent manner. To our knowledge, this is the first report demonstrating that fluvoxamine binds to sigma-1 receptors in the living human brain at therapeutic doses, which is consistent with the previous report using rat brain (3). Suhara *et al.* (38) reported a high occupancy (approximately 80%) of serotonin transporters in healthy subjects after a single oral administration of fluvoxamine (50 mg). These results suggest that, at therapeutic doses, fluvoxamine binds to sigma-1 receptors as well as serotonin transporters in the human brain. Taken together, these results suggest that sigma-1 receptors may be involved in the mechanism of the action of fluvoxamine.

A recent study demonstrated that cognitive deficits induced in mice by the N-methyl-D-aspartate receptor antagonist phencyclidine (PCP) could be ameliorated by subsequent subchronic administration of fluvoxamine, and that the effects of fluvoxamine could be antagonized by co-administration of the selective sigma-1 receptor antagonist NE-100 (20). Furthermore, the selective sigma-1 receptor agonist SA4503 and the endogenous sigma-1 receptor agonist dehydroepiandrosterone sulphate could improve PCP-induced cognitive deficits in mice, and the efficacy of SA4503 and dehydroepiandrosterone-sulphate on PCP-in-

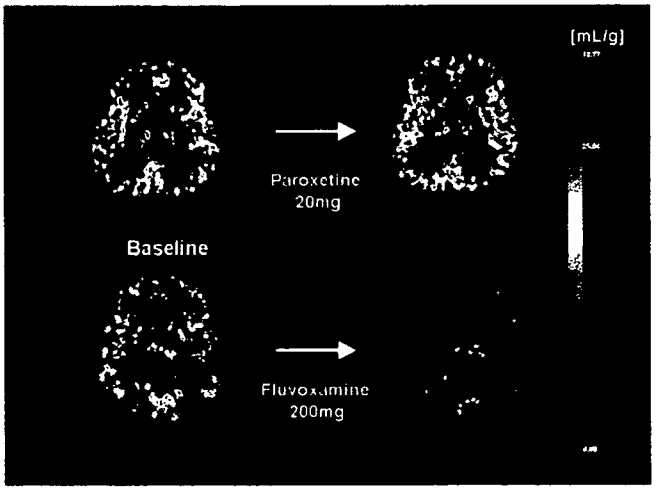

Figure 2. Distribution volume images of [^{11}C]SA4503-PET before and after a single oral administration of an SSRI. The upper pair represents distribution volume images at baseline (left) and at paroxetine (20 mg)-loading (right) in the same subject. The lower pair shows distribution volume images at baseline (left) and fluvoxamine (200 mg)-loading (right) in another subject. PET, positron emission tomography; SSRI, selective serotonin reuptake inhibitor.

Table 1. Binding potential of [^{11}C]SA4503 and occupancy (%) of selective serotonin reuptake inhibitors in the human brain regions

	Frontal Cortex		Temporal Cortex		Parietal Cortex		Occipital Cortex	
	Baseline	SSRI	Baseline	SSRI	Baseline	SSRI	Baseline	SSRI
F50								
Binding potential	15.9±5.2	10.0±3.0	19.5±6.1	14.0±6.0	15.3±4.3	9.57±3.0	14.7±4.8	10.1±4.5
Occupancy (%)	35.5±11.8		27.3±20.0		36.2±13.9		30.8±19.3	
F100								
Binding potential	11.7±3.0	6.56±0.1	14.3±2.6	8.93±2.7	13.6±1.7	7.10±1.2	12.9±0.9	6.69±0.8
Occupancy (%)	41.7±13.0		36.1±22.6		47.0±12.8		48.0±7.3	
F150								
Binding potential	20.9±3.7	7.50±1.2	26.9±4.9	10.0±1.0	20.6±1.9	7.39±0.5	19.2±5.3	6.86±0.3
Occupancy (%)	62.8±12.7		61.7±8.6		63.8±5.9		62.3±10.7	
F200								
Binding potential	17.0±5.1	6.35±0.1	20.8±7.0	9.89±2.9	16.7±4.4	6.27±0.4	15.0±6.0	5.18±1.0
Occupancy (%)	59.9±13.6		50.2±14.9		59.9±14.5		63.0±11.5	
P20								
Binding potential	16.5±2.9	17.1±1.6	20.9±5.6	20.6±1.2	18.4±3.6	15.7±2.2	15.6±3.5	14.8±3.0
Occupancy (%)	−4.40±9.1		−2.2±22.1		13.8±5.6		4.70±4.8	

Value are the mean ± SD of three subjects.

F50, Fluvoxamine (50 mg); F100, fluvoxamine (100 mg); F150, fluvoxamine (150 mg); F200, fluvoxamine (200 mg); P20, paroxetine (20 mg); SSRI, fluvoxamine or paroxetine.

duced cognitive deficits was also antagonized by co-administration of NE-100 (20). These findings suggest that the agonistic activity of fluvoxamine at sigma-1 receptors could be implicated in the mechanisms of the action of fluvoxamine (20). Therefore, the agonistic property of fluvoxamine at sigma-1 receptors may suggest that this drug has potential for the treatment of cognitive deficits in depressive and schizophrenic patients.

Mood disorders, including major depressive disorder and bipolar disorder, possess cognitive impairment in the center of their psychopathology. There is a hypothesis that cognitive dysfunction remains after remission, especially in manic bipolar disorder (39), and leads to poor social outcome. As suggested, fluvoxamine may have a potential for treating cognitive deficits through its action against sigma-1 receptors, it being an antidepressant, fluvoxamine may be a useful prescription for mood disorders having cognitive impairment.

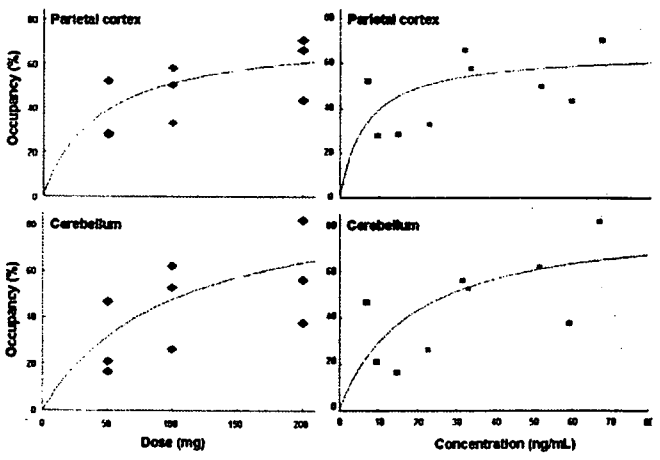

Figure 3. Correlations between the sigma-1 receptor occupancy and dose or blood concentration of fluvoxamine in the parietal cortex and cerebellum. The colors of the points correspond to the dose administered.

An adjunct medication is often added to antipsychotic treatment regimens to improve the response of negative symptoms and cognitive deficits in schizophrenia. Some SSRIs, such as fluvoxamine and fluoxetine, can ameliorate primary negative symptoms in chronic schizophrenic patients (40,41). Currently, the precise mechanism(s) underlying the efficacy of fluvoxamine on negative symptoms is unclear. However, it is possible that sigma-1 receptors play a role in the mechanism of the action of fluvoxamine, although further study will be needed to confirm this. Taken together, these results also suggest that augmentation with sigma-1 receptor agonists such as fluvoxamine could be a useful addition to the treatment of schizophrenic patients with persistent negative symptoms and cognitive deficits.

Psychotic major depression is a difficult-to-treat illness that is associated with high functional impairment and significantly higher mortality than nonpsychotic major depression (42,43). Interestingly, monotherapy of fluvoxamine has been proven effective against both the psychotic and depressive symptoms of this disorder (44–46). In contrast, a monotherapy of paroxetine did not show equal efficacy as fluvoxamine (47). Based on these findings, it has been recently proposed that this efficacy of fluvoxamine might be due to its specific affinity to sigma-1 receptors in the brain (48,49), suggesting that sigma-1 receptors play a role in psychotic major depression. Therefore, it may be interesting to study whether the binding of [^{11}C]SA4503 to sigma-1 receptors in the brain is altered in patients with psychotic major depression.

Miyatake *et al.* (30) reported functional polymorphisms (T-485A) in the promoter region of the SIGMAR1 gene. In this study, we found that there was no association between the SIGMAR1 genotype and the binding potentials of [^{11}C]SA4503 in any of the regions of the brain in healthy male subjects. These findings suggest that the SIGMAR1 gene polymorphism GC-241-240TT may not contribute to differences in the sigma-1 receptors in the human brain, although a further study using a larger sample will be necessary.

In conclusion, the present study demonstrates that fluvoxamine binds to sigma-1 receptors in the human brain at therapeutic

Table 1. (continued)

Anterior Cingulate Gyrus		Head of Caudate Nucleus		Putamen		Thalamus		Cerebellum	
Baseline	SSRI	Baseline	SSRI	Baseline	SSRI	Baseline	SSRI	Baseline	SSRI
18.3±6.1	11.5±2.6	13.8±3.8	9.32±2.2	14.1±4.3	9.06±1.9	16.4±6.4	11.1±3.5	23.5±8.5	16.5±6.5
34.0±17.6		31.2±11.2		34.0±8.8		29.1±15.1		28.2±16.3	
15.3±4.0	8.38±1.4	12.3±0.8	6.19±0.3	12.6±1.5	6.05±0.4	13.7±1.4	8.21±0.4	20.3±6.6	10.1±2.4
40.1±28.9		49.6±1.9		51.7±4.0		39.6±9.1		47.1±18.5	
22.2±3.0	9.23±1.6	17.4±0.4	6.05±2.3	18.6±2.3	7.88±1.3	17.8±1.6	8.57±1.0	29.6±8.5	9.88±1.9
58.1±10.0		65.1±14.2		56.7±12.1		52.4±8.1		65.5±6.9	
19.9±6.0	7.11±1.2	14.3±3.4	5.01±1.0	15.5±5.7	6.11±1.1	14.9±4.4	6.16±1.1	22.8±8.4	8.22±2.4
61.7±14.0		62.1±18.7		55.8±20.5		57.1±8.9		58.5±22.2	
18.0±4.6	18.4±3.8	15.5±2.9	15.0±5.1	16.8±4.4	15.5±1.5	14.7±3.0	15.9±3.1	23.3±6.8	23.7±1.9
−5.20±26.8		5.10±14.4		5.43±14.2		−11.7±35.3		−7.15±28.7	

doses. These findings suggest that sigma-1 receptors may play an important role in the mechanism of action of fluvoxamine. 26,33

This study was supported in part by a grant from the Program for Promotion of Fundamental Studies in Health Sciences of the National Institute of Biomedical Innovation, Japan (to KH and KI, No: 06-46). Dr. Hashimoto reports having received the speakers' bureau honoraria from Solvay Pharmaceuticals. Drs. Ishikawa, Ishiwata, Ishii, Kimura, Sakata, Naganawa, Oda, Miyatake, Fujisaki, Shimizu, Shirayama, and Iyo report no competing interests.

We thank Dr. Masaya Hashimoto and Ms. Hiroko Tsukinari for technical assistance.

Supplementary material cited in this article is available online.

1. Owens MJ (2004): Selectivity of antidepressants: from the monoamine hypothesis of depression to the SSRI revolution and beyond. *J Clin Psychiatry* 65:5–10.
2. Millan ML (2006): Multi-target strategies for the improved treatment of depressive states: Conceptual foundations and neuronal substrates, drug discovery and therapeutic application. *Pharmacol Ther* 110:135–370.
3. Narita N, Hashimoto K, Tomitaka S, Minabe Y (1996): Interactions of selective serotonin reuptake inhibitors with subtypes of sigma receptors in rat brain. *Eur J Pharmacol* 307:117–119.
4. Goodnick PJ, Goldstein BJ (1998): Selective serotonin reuptake inhibitors in affective disorders–I. Basic pharmacology. *J Psychopharmacol* 12:S5–20.
5. Goodnick PJ, Goldstein BJ (1998): Selective serotonin reuptake inhibitors in affective disorders–II. Efficacy and quality of life. *J Psychopharmacol* 12:S21–54.
6. Stahl SM (1998): Not so selective serotonin selective reuptake inhibitors. *J Clin Psychiatry* 59:343–344.
7. Stahl SM (1998): Using secondary binding properties to select a not so selective serotonin selective reuptake inhibitor. *J Clin Psychiatry* 59:642–643.
8. Nemeroff CB, Owens MJ (2004): Pharmacologic differences among the SSRIs: focus on monoamine transporters and the HPA axis. *CNS Spectr* 9:23–31.
9. Bermack JE, Debonnel G (2005): The role of sigma receptors in depression. *J Phamacol Sci* 97:317–336.
10. Carrasco JL, Sandner C (2005): Clinical effects of pharmacological variations in selective serotonin reuptake inhibitors: An overview. *Int J Clin Pract* 59:1428–1434.
11. Westenberg HGM, Sandner C (2006): Tolerability and safety of fluvoxamine and other antidepressants. *Int J Clin Pract* 60:482–491.
12. Walker JM, Bowen WD, Walker FO, Matsumoto RR, De Costa B, Rice KC (1990). Sigma receptors: Biology and function. *Pharmacol Rev* 42:355–402.
13. Maurice T, Urani A, Phan VL, Romieu P (2001): The interaction between neuroactive steroids and the sigma-1 receptor function: Behavioral consequences and therapeutic opportunities. *Brain Res Rev* 37:116–132.
14. Hayashi T, Su TP (2004): Sigma-1 receptor ligands: potential in the treatment of neuropsychiatric disorders. *CNS Drugs* 18:269–284.
15. Hashimoto K, Ishiwata K (2006): Sigma receptor ligands: Possible application as therapeutic drugs and as radiopharmaceuticals. *Curr Pharm Des* 12:3857–3876.
16. Monnet FP, Maurice T (2006): The sigma-1 protein as a target for the nongenomic effects of neuro(active)steroids: Molecular, physiological, and behavioral aspects. *J Pharmacol Sci* 100:93–118.
17. Hayshi T, Su TP (2005): The potential role of sigma-1 receptors in lipid transport and lipid raft reconstitution in the brain: Implication for drug abuse. *Life Sci* 77:1612–1624.
18. Hayashi T, Maurice T, Su TP (2000): Ca^{2+} signaling via sigma-1 receptors: novel regulatory mechanism affecting intracellular Ca^{2+} concentration. *J Pharmacol Exp Ther* 293:788–798.
19. Hayashi T, Su TP (2001): Regulating ankyrin dynamics: Roles of sigma-1 receptors. *Proc Natl Acad Sci U S A* 98:491–496.
20. Hashimoto K, Fujita Y, Iyo M (2007): Phencyclidine-induced cognitive deficits in mice are improved by subsequent subchronic administration of fluvoxamine: Role of sigma-1 receptors. *Neuropsychopharmacology* 32:514–521.
21. Waarde A (2000): Measuring receptor occupancy with PET. *Curr Pharm Des* 6:1593–1610.
22. Kapur S, Seeman P (2001): Does fast dissociation from the dopamine D_2 receptor explain the action of atypical antipsychotics?: A new hypothesis. *Am J Psychiatry* 158:360–369.
23. Kawamura K, Ishiwata K, Tajima H, Ishii S, Matsuno K, Homma Y, *et al.* (2000): In vivo evaluation of [^{11}C]SA4503 as a PET ligand for mapping CNS sigma-1 receptors. *Nucl Med Biol* 27:255–261.
24. Kawamura K, Elsinga PH, Kobayashi T, Ishii S, Wang WF, Matsuno K, *et al.* (2003): Synthesis and evaluation of ^{11}C- and ^{18}F-labeled 1-[2-(4-alkoxy-3-methoxyphenyl)ethyl]-4-(3-phenylpropyl)piperazines as sigma receptor ligands for positron emission tomography studies. *Nucl Med Biol* 30:273–284.

25. Ishiwata K, Tsukada H, Kawamura K, Kimura Y, Nishiyama S, Kobayashi T, *et al.* (2001): Mapping of CNS sigma-1 receptors in the conscious monkey: Preliminary PET study with [^{11}C]SA4503. *Synapse* 40:235–237.
26. Ishiwata K, Kawamura K, Kobayashi T, Matsuno K (2003): Sigma-1 and dopamine D_2 receptor occupancy in the mouse brain after a single administration of haloperidol and two dopamine D_2-like receptor ligands. *Nucl Med Biol* 30:429–434.
27. Matsuno K, Nakazawa M, Okamoto K, Kawashima Y, Mita S (1996): Binding properties of SA4503 a novel and selective sigma1 receptor agonist. *Eur J Pharmacol* 306:271–279.
28. Mishina M, Ishiwata K, Ishii K, Kitamura S, Kimura Y, Kawamura K, *et al.* (2005): Function of sigma-1 receptors in Parkinson's disease. *Acta Neurol Scand* 112:103–107.
29. Ishiwata K, Oda K, Sakata M, Kimura Y, Kawamura K, Oda K, *et al.* (2006): A feasible study of [^{11}C]SA4503-PET for evaluating sigma-1 receptor occupancy by neuroleptics: The binding of haloperidol to sigma-1 and dopamine D_2-like receptors. *Ann Nucl Med* 20:569–573.
30. Miyatake R, Furukawa A, Matsushita S, Higuchi S, Suwaki H (2004): Functional polymorphisms in the sigma-1 receptor gene associated with alcoholism. *Biol Psychiatry* 55:85–90.
31. de Vries MH, Raghoebar M, Mathlener IS, van Harten J (1992): Single and multiple oral dose fluvoxamine kinetics in young and elderly subjects. *Ther Drug Monit* 14:493–498.
32. de Vries MH, van Harten J, van Bemmel P, Raghoebar M (1993): Pharmacokinetics of fluvoxamine maleate after increasing single oral doses in healthy subjects. *Biopharm Drug Dispos* 14:291–296.
33. Fujiwara T, Watanuki S, Yamamoto S, Miyake M, Seo S, Itoh M, *et al.* (1997): Performance evaluation of a large axial field-of-view PET scanner: SET-2400W. *Ann Nucl Med* 11:307–313.
34. Sakata M, Kimura Y, Naganawa M, Oda K, Ishii K, Chihara K, *et al.* (2007): Mapping of human cerebral sigma-1 receptors using positron emission tomography and [^{11}C]SA4503. *Neuroimage* 35:1–8.
35. Mintun MA, Raichle ME, Kilbourn MR, Wooten GF, Welch MJ (1984): A quantitative model for the in vivo assessment of drug binding sites with positron emission tomography. *Ann Neurol* 15:217–227.
36. Logan J, Fowler JS, Volkow ND, Wang GJ, Ding YS, Alexoff DL (1996): Distribution volume ratios without blood sampling from graphical analysis of PET data. *J Cereb Blood Flow Metab* 16:834–840.
37. Ishiguro H, Ohtsuki T, Toru M, Itokawa M, Aoki J, Shibuya H, *et al.* (1998): Association between polymorphisms in the type 1 sigma receptor gene and schizophrenia. *Neurosci Lett* 257:45–48.
38. Suhara T, Takano A, Sudo Y, Ichimiya T, Inoue M, Yasuno F, *et al.* (2003): High levels of serotonin transporter occupancy with low-dose clomipramine in comparative occupancy study with fluvoxamine using positron emission tomography. *Arch Gen Psychiatry* 60:386–391.
39. Gruber S, Rathgeber K, Braunig P, Gauggel S (2007): Stability and course of neuropsychological deficits in manic and depressed bipolar patients compared to patients with major depression. *J Affect Disord* Mar 13; [Epub ahead of print].
40. Silver H (2003): Selective serotonin reuptake inhibitor augmentation in the treatment of negative symptoms of schizophrenia. *Int Clin Psychopharmacol* 18:305–313.
41. Silver H (2004): Selective serotonin re-uptake inhibitor augmentation in the treatment of negative symptoms of schizophrenia. *Expert Opin Pharmacother* 5:2053–2058.
42. Schatzberg AF (2003): New approaches to managing psychotic depression. *J Clin Psychiatry* 64:19–23.
43. Vythilingam M, Chen J, Bremner JD, Mazure CM, Maciejewski PK, Nelson JC (2003): Psychotic depression and mortality. *Am J Psychiatry* 160:574–576.
44. Gatti F, Bellini L, Gasperini M, Perez J, Zanardi R, Smeraldi E (1996): Fluvoxamine alone in the treatment of delusional depression. *Am J Psychiatry* 153:414–416.
45. Hirschfeld RM (1999): Efficacy of SSRIs and newer antidepressants in severe depression: Comparison with TCAs. *J Clin Psychiatry* 60:326–335.
46. Zanardi R, Franchini L, Gasperini M, Lucca A, Smeraldi E, Perez J (1998): Faster onset of action of fluvoxamine in combination with pindolol in the treatment of delusional depression: A controlled study. *J Clin Psychopharmacol* 18:441–446.
47. Zanardi R, Franchini L, Gasperini M, Perez J, Smeraldi E (1996): Double-blind controlled trial of sertraline versus paroxetine in the treatment of delusional depression. *Am J Psychiatry* 153:1631–1633.
48. Stahl SM (2005): Antidepressant treatment of psychotic major depression: Potential role of the σ receptor. *CNS Spectr* 10:319–323.
49. Hayashi T, Su TP (2005): Understanding the role of sigma-1 receptors in psychotic depression. *Psychiatric Times* 22:54–63.

SYNAPSE 61:778–784 (2007)

Evaluation of Distribution of Adenosine A_{2A} Receptors in Normal Human Brain Measured With [^{11}C]TMSX PET

MASAHIRO MISHINA,[1,2,3]* KIICHI ISHIWATA,[2] YUICHI KIMURA,[2] MIKA NAGANAWA,[2,4] KEIICHI ODA,[2] SHIRO KOBAYASHI,[1] YASUO KATAYAMA,[3] AND KENJI ISHII[2]

[1]*Neurological Institute, Nippon Medical School Chiba-Hokusoh Hospital, Imba-gun, Chiba-ken 270-1694, Japan*
[2]*Positron Medical Center, Tokyo Metropolitan Institute of Gerontology, Itabashi-ku, Tokyo 173-0022, Japan*
[3]*The Second Department of Internal Medicine, Nippon Medical School, Bunkyo-ku, Tokyo 113-8602, Japan*
[4]*JSPS Research Fellow, Japan Society for the Promotion of Science, Chiyoda-ku, Tokyo 102-8471, Japan*

KEY WORDS adenosine A_{2A} receptor; positron emission tomography; [^{11}C]TMSX; human brain; Parkinson's disease

ABSTRACT Adenosine A_{2A} receptor (A2AR) is thought to interact with dopamine D_2 receptor. Selective A2AR antagonists have attracted attention as the treatment of Parkinson's disease. In this study, we investigated the distribution of the A2ARs in the living human brain using positron emission tomography (PET) and [7-methyl-^{11}C]-(*E*)-8-(3,4,5-trimethoxystyryl)-1,3,7-trimethylxanthine ([^{11}C]TMSX). We recruited five normal male subjects. A dynamic series of PET scans was performed for 60 min, and the arterial blood was sampled during the scan to measure radioactivity of the parent compound and labeled metabolites. Circular regions of interest of 10-mm diameter were placed in the PET images over the cerebellum, brainstem, thalamus, head of caudate nucleus, anterior and posterior putamen, frontal lobe, temporal lobe, parietal lobe, occipital lobe, and posterior cingulate gyrus for each subject. A two-tissue, three-compartment model was used to estimate K_1, k_2, k_3, and k_4 between metabolite-corrected plasma and tissue time activity of [^{11}C]TMSX. The binding potential (BP) was the largest in the anterior (1.25) and posterior putamen (1.20), was next largest in the head of caudate nucleus (1.05) and thalamus (1.03), and was small in the cerebral cortex, especially frontal lobe (0.46). [^{11}C]TMSX PET showed the largest BP in the striatum in which A2ARs were enriched as in postmortem and nonhuman studies reported, but that the binding of [^{11}C]TMSX was relatively larger in the thalamus to compare with other mammals. To date, [^{11}C]TMSX is the only promising PET ligand, which is available to clinical use for mapping the A2ARs in the living human brain. **Synapse 61:778–784, 2007.** ©2007 Wiley-Liss, Inc.

INTRODUCTION

Adenosine is produced by conversion of intra- and extracellular adenine nucleotides (Latini and Pedata, 2001), and plays a role as an endogenous modulator of synaptic functions in the central nervous system (Dunwiddie and Masino, 2001). The effects are mediated by at least four receptor subtypes: A_1, A_{2A}, A_{2B}, and A_3 (Fredholm et al., 2001). The adenosine A_{2A} receptors are enriched in dopamine-rich areas of the brain, such as the basal ganglia (Fredholm and Svenningsson, 2003), while adenosine A_1 receptors are widely distributed throughout the entire brain (Fukumitsu et al., 2005). The adenosine A_{2A} receptors are known to stimulate adenyl cyclase and would interact with dopamine D_2 receptor negatively at the level of second messengers and beyond (Fredholm and Svenningsson, 2003). For example, high-affinity binding of a dopamine D_2 agonist could be reduced by stimulation of adenosine A_{2A} receptors (Ferre et al., 1991).

Recently, adenosine A_{2A} receptor antagonists have attracted attention as the nondopaminergic treatment of Parkinson's disease. Caffeine is a nonselective adenosine receptor antagonist and is known to reduce the risk of developing Parkinson's disease (Ascherio et al., 2001; Ross et al., 2000). Theophylline, which is also a nonselective antagonist, was expected as a promising

Contract grant sponsor: Japan Society for the Promotion of Science; Contract grant numbers: No 16390348, No. 17590901.

*Correspondence to: Masahiro Mishina, MD, Neurological Institute, Nippon Medical School Chiba-Hokusoh Hospital, 1715 Kamagari, Imba-mura, Imba-gun, Chiba-ken 270-1694, Japan. E-mail: mishina@nms.ac.jp

Received 17 November 2006; Accepted 26 March 2007

DOI 10.1002/syn.20423

Published online 13 June 2007 in Wiley InterScience (www.interscience.wiley.com).

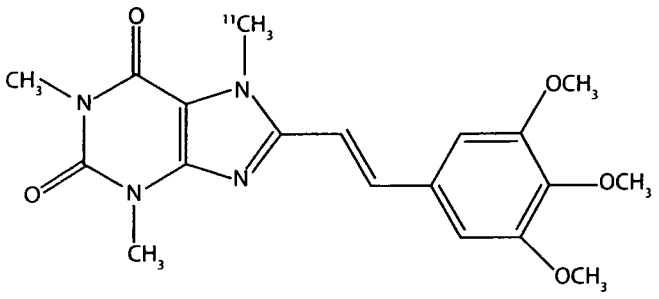

Fig. 1. Chemical structure of [^{11}C]TMSX.

agent of Parkinson's disease (Kostic et al., 1999). However, clinical trials of the caffeine and theophylline have been unimpressive (Kulisevsky et al., 2002; Schwarzschild et al., 2002). The selective adenosine A_{2A} receptor antagonist, istradefylline (KW6002), has been developed as a novel nondopaminergic agent for Parkinson's disease (Kase, 2001), and provides an antiparkinsonian benefit without causing and worsening dyskinesia that is one of the most inconvenient side effects of dopaminergic therapy (Bara-Jimenez et al., 2003). A postmortem study suggested that adenosine A_{2A} receptors was increased in the patients with dyskinesia following long-term levodopa therapy (Calon et al., 2004). Therefore, adenosine A_{2A} receptors may be involved with the appearance of the side effects of the antiparkinsonian agents.

Although adenosine A_{2A} receptor has attracted much attention, little information was available about the receptor in the living human brain until quite recently. However, we developed a PET ligand, [7-methyl-^{11}C]-(*E*)-8-(3,4,5-trimethoxystyryl)-1,3,7-trimethylxanthine ([^{11}C]TMSX, Fig. 1), for mapping the adenosine A_{2A} receptors (Ishiwata et al., 2000a,b, 2002). Preliminarily, we have successfully visualized the receptors in a living human brain in comparison with distribution of adenosine A_1 receptors and dopamine D_2 receptors, and the receptor-specific binding of [^{11}C]TMSX was confirmed by theophylline challenge (Ishiwata et al., 2005). The aim of this study is to establish the measurement of the adenosine A_{2A} receptors in the living human brain using the [^{11}C]TMSX PET, and to compare with the results of past postmortem and nonhuman studies.

MATERIALS AND METHODS

Subjects

We recruited five-normal male subjects, without the history of neurological disease or any abnormalities on physical or neurological examinations (mean age ± SD, 23.0 ± 3.3). They were all right-handed. They had neither medication known to affect the brain function nor history of alcoholism.

The study protocols were approved by the Ethics Committee of Tokyo Metropolitan Institute of Gerontology. A written informed consent was obtained from all of the subjects who participated in this study.

Magnetic resonance imaging

Magnetic resonance images (MRI) were obtained with the spoiled gradient-recalled echo in steady state technique and a SIGNA 1.5 Tesla machine (General Electric, Waukesha, WI). MRI images were examined for any organic abnormalities in the subjects' brain, and were used as a reference for placing regions of interest (ROIs) on PET images.

Positron emission tomography imaging

PET was performed in the Tokyo Metropolitan Institute of Gerontology Positron Medical Center with an SET-2400W PET scanner (Shimadzu Co., Kyoto, Japan) (Fujiwara et al., 1997). [^{11}C]TMSX was prepared as described before (Ishiwata et al., 2003). Specific activity at the time of injection ranged from 12.8 to 48.9 GBq/μmol (27.4 ± 14.5 GBq/μmol). After transmission scan with a rotating ^{68}Ga/^{68}Ge line source to correct for the photon attenuation using the attenuation map, a dynamic series of decay-corrected PET data acquisition was performed for 60 min starting at the time of 500 MBq of [^{11}C]TMSX injection. The total number of frames was 27, and the frame arrangements were 10 s × 6, 30 s × 3, 1 min × 5, 2.5 min × 5, 5 min × 8. Arterial blood was sampled at 10, 20, 30, 40, 50, 60, 70, 80, 90, 100, 110, 120, 135, and 150 s, and at 3, 5, 7, 10, 15, 20, 30, 40, 50, and 60 min. Plasma was separated, weighed, and measured for radioactivity with an NaI (Tl) well scintillation counter. Metabolite analysis was carried out by high-performance liquid chromatography (HPLC). The time activity curves in plasma (pTAC) were expressed as standardized uptake value (SUV, [Bq/ml tissue]/[Bq dose/g body weight]). All procedures were performed under dim light to prevent photoisomerization of the TMSX (Ishiwata et al., 1996, 2000a, 2003).

Kinetic analysis

We generated early images by adding up frames of the dynamic scan from 0 to 10 min (Mishina et al., 2000). The MRI was three-dimensionally registered to the early image of each subject using the K-means clustering algorithm (Ardekani et al., 1995). Using a medical image processing application package "Dr. View" version 5.2 (AJS Co., Tokyo, Japan), the early images and the registered MRI images were used as a reference for placing ROIs on PET image of dynamic scans (Fig. 2). Circular ROIs of 10-mm diameter and extending over two slices of the PET images were drawn on the cerebellum, brainstem, thalamus, head of caudate nucleus, anterior and posterior putamen, frontal lobe, temporal lobe, parietal lobe, occipital lobe, and posterior cingulate gyrus. We also placed the ROIs

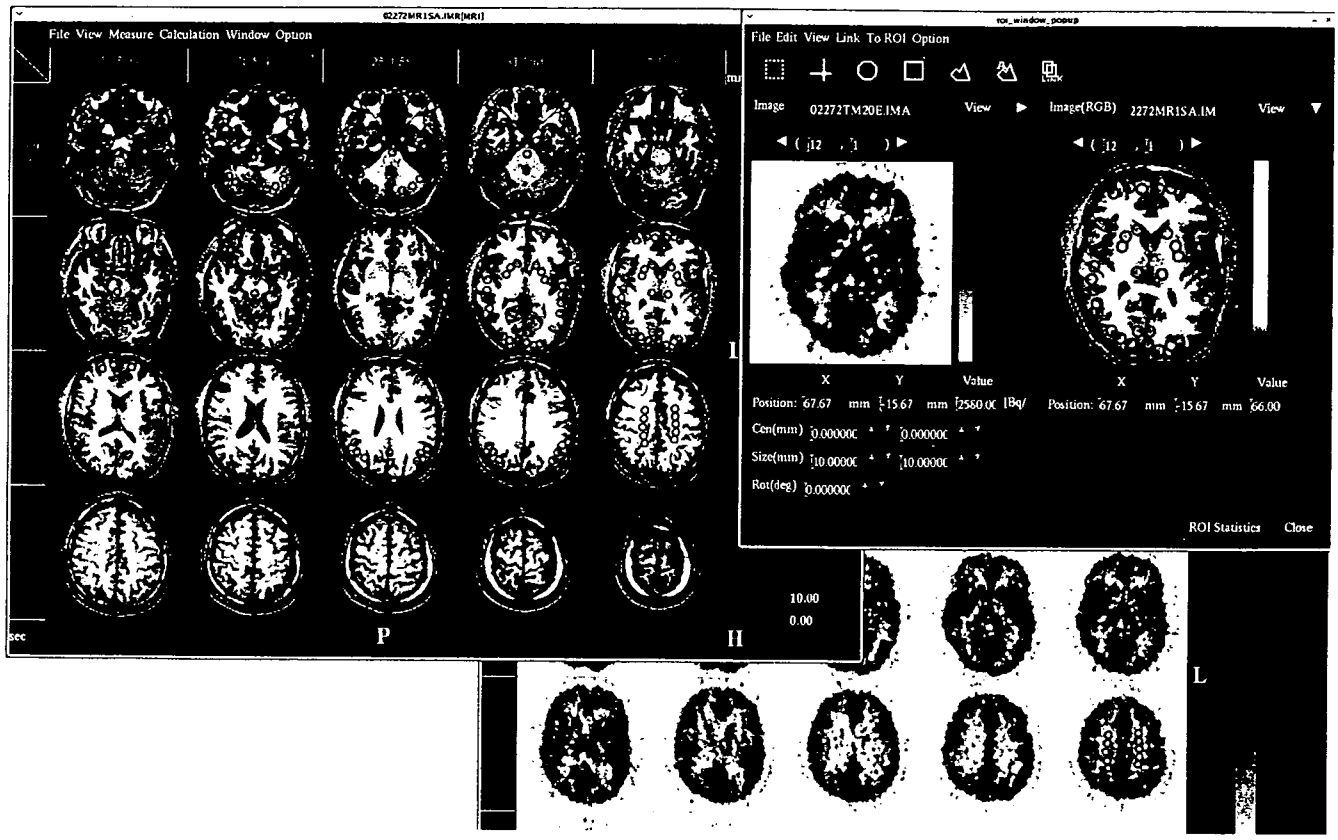

Fig. 2. Placement of regions of interest using Dr. View. Using the software, we can place the same ROIs on the images of different modalities.

over the centrum semiovale on one slice as a reference region for kinetic analysis. Time activity curves in tissue (tTACs) were calculated as SUV with the dynamic data and ROIs. A kinetic analysis of the tTACs was performed using programs implemented on MATLAB 7.04 (The Mathworks, Natick, MA). The metabolite-corrected pTAC was used as an input function. A two-tissue, three-compartment model was used to estimate K_1, k_2, k_3, and k_4 between pTAC and tTAC of [^{11}C]TMSX using Gauss-Newton algorithm (Kawamura et al., 2003) and a tTAC of the centrum semiovale. Estimation of delay was performed in a round-robin fashion (Kimura et al., 2004). Then, total distribution volume (DVt), $\frac{K_1}{k_2}\left(1+\frac{k_3}{k_4}\right)$, and binding potential (BP), $\frac{k_3}{k_4}$, were calculated using the parameters. Rate of specific binding (SB) was calculated as $\frac{BP}{DVt}$. Parametric images of DVt for [^{11}C]TMSX were also generated using a graphical analysis (Logan, 2003). Rationale of the kinetic analysis was validated in detail by Naganawa et al. (2007).

RESULTS

Figure 3 demonstrate the curve for the unmetabolized [^{11}C]TMSX and the unmetabolized ratio of [^{11}C]TMSX in plasma, respectively. The radioactivity level in plasma rapidly decreased for the first 5 min (Fig. 3A). [^{11}C]TMSX was metabolically stable in plasma, and over 90% of the radioactivity remained as the intact form for 60 min (Fig. 3B).

Figure 4 demonstrates the time radioactivity curve in the putamen, frontal cortex, and centrum semiovale. [^{11}C]TMSX was taken at high level, and the uptake reached a peak at 1.5–2.5 min after injection, followed by a gradual decrease. The SUV was large in the putamen and small in the frontal lobe.

Figure 5 shows representative parametric images for the DVt of [^{11}C]TMSX. The images demonstrate that the DVt was high in the putamen, head of caudate nucleus and thalamus, and was low in the cerebral cortex.

The BP was large in the anterior and posterior putamen, head of caudate nucleus and thalamus, was moderate in the cerebellum and brainstem, and was small in the cerebral cortices, especially frontal lobe (Table I). The rate of specific binding was 62% in the putamen and 38% in the frontal cortex (Table I).

DISCUSSION

Our study demonstrated that adenosine A_{2A} receptors in human brain were enriched in the striatum, as

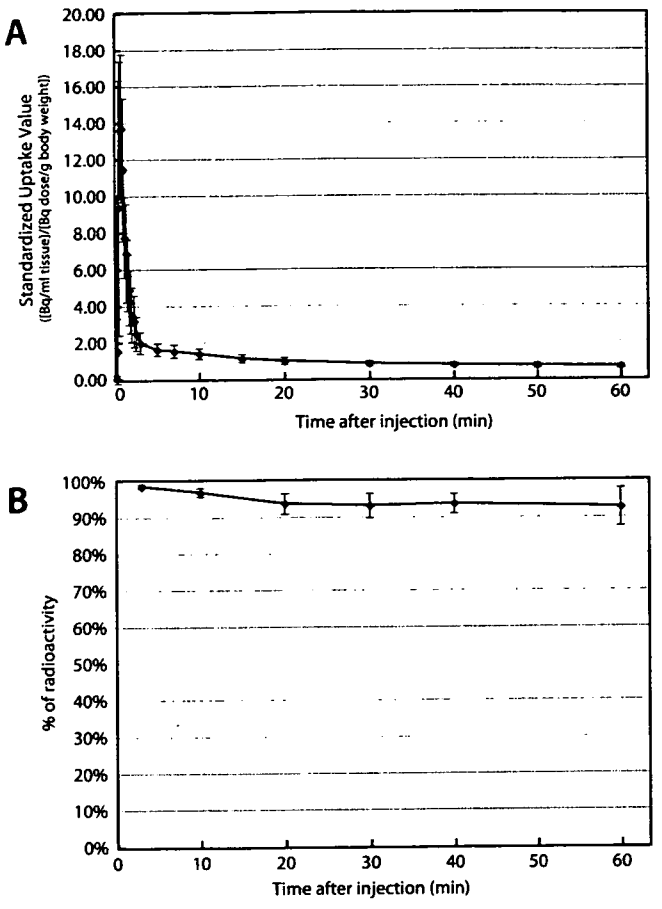

Fig. 3. Decay-corrected time–radioactivity curve for unmetabolized [^{11}C]TMSX in plasma (**A**) and unmetabolized ratio of [^{11}C]TMSX (**B**). Data represent means and SD of five subjects.

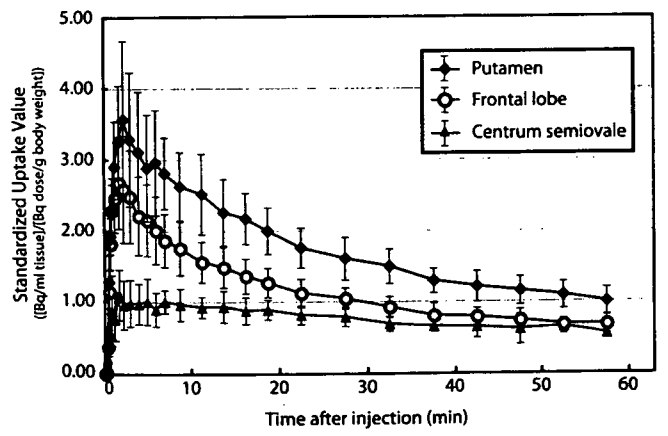

Fig. 4. Decay-corrected time–radioactivity curve for unmetabolized [^{11}C]TMSX in the putamen, frontal cortex, and centrum semiovale for five normal subjects.

well as human postmortem studies (Martinez-Mir et al., 1991; Svenningsson et al., 1997). Among the mouse, rat, and monkey studies using [^{11}C]TMSX (Ishiwata et al., 2000a) and [^{11}C]SCH44241 (Moresco

Fig. 5. A parametric image for the total distribution volume of [^{11}C]TMSX generated using a graphical analysis. This image is including the nonspecific binding of TMSX. The image demonstrate that the distribution of [^{11}C]TMSX was high in the putamen, head of caudate nucleus and thalamus, and low in the cerebral cortex.

TABLE I. Total distribution volume, binding potential, and rate of specific binding of [^{11}C]TMSX

	DVt (ml/mg)	BP	SB (%)
Cerebellum	1.39 ± 0.34	0.85 ± 0.15	53.0 ± 2.8
Brainstem	1.33 ± 0.31	0.77 ± 0.13	50.7 ± 3.3
Thalamus	1.53 ± 0.37	1.03 ± 0.13	58.0 ± 1.8
Caudate nucleus	1.55 ± 0.36	1.05 ± 0.17	58.4 ± 3.5
Anterior putamen	1.69 ± 0.38	1.25 ± 0.17	62.7 ± 3.5
Posterior putamen	1.66 ± 0.41	1.20 ± 0.16	61.8 ± 2.3
Frontal lobe	1.10 ± 0.27	0.46 ± 0.11	37.8 ± 3.3
Temporal lobe	1.16 ± 0.27	0.54 ± 0.11	42.1 ± 3.5
Occipital lobe	1.17 ± 0.26	0.56 ± 0.10	42.7 ± 3.9
Parietal lobe	1.14 ± 0.26	0.51 ± 0.10	40.6 ± 3.3
Posterior cingulate gyrus	1.29 ± 0.30	0.72 ± 0.14	49.0 ± 4.0

DVt = total distribution volume, BP = binding potential, SB = rate of specific binding.

et al., 2005), which is also a selective adenosine A_{2A} receptor antagonist, the uptake of the tracer was higher in the striatum than in the other brain region. The findings are coincident with the fact that the adenosine A_{2A} receptors are enriched in the striatum in all species.

Our study showed that the distribution of the adenosine A_{2A} receptors were widespread other than in striatum. Following in the putamen and head of caudate nucleus, the BP of [^{11}C]TMSX was the largest in the thalamus. The BP was smaller in the cerebral cortex, especially frontal lobe, than in the cerebellum. Table II summarizes previous works for bindings pf radioligands to adenosine A_{2A} receptors in experimental animals. [^{11}C]TMSX uptake was lower in the cerebral cortex than in the cerebellum (Ishiwata et al., 2000a). The animal study using [^{11}C]SCH44241 reported, however, that the uptake was higher in the cerebral cortex than in the cerebellum (Moresco et al., 2005). The postmortem study revealed that the density of adenosine A_{2A} receptors in the putamen and caudate nucleus was five times of that in the thalamus, and was 3~5 times of those in the cortices (Svenningsson et al., 1997). Our result showed, however, that the BP of [^{11}C]TMSX in the putamen was 1.2

TABLE II. Summary of past studies on the binding of radioligands to adenosine A_{2A} receptors

	Description						
	Uptake ratio				BP (mean ± SD)	B_{MAX} ± SEM (fmol/mg)	Reference
	5 min	15 min	30 min	60 min			
[^{11}C]TMSX							
Mouse: in vitro autoradiography							
Striatum/cortex	2.32	2.82	2.85	2.53			Ishiwata et al., 2000a*
Striatum/cerebellum	2.08	2.71	2.64	2.55			
Rat: in vitro autoradiography							
Striatum/cortex		3.16					
Striatum/cerebellum		2.67					
Monkey: PET							
Striatum/cortex	1.30	1.40	1.47	1.56			
Striatum/cerebellum	1.20	1.22	1.26	1.46			
[^{11}C]SCH44241							
Monkey: PET							
Striatum					0.74 ± 0.02		Moresco et al., 2005
Cortex					0.16 ± 0.04		
Cerebellum					0.13 ± 0.06		
[^{3}H]SCH58261							
Postmorten human: in vitro autoradiography							
Rostral putamen						15.0 ± 1.5	Svenningsson et al., 1997
Caudal putamen						11.2 ± 0.9	
Frontal cortex						5.2 ± 0.8	
Occiptal cortex						3.4 ± 1.0	
Medial nucleus of thalamus						3.7 ± 1.0	

*[^{11}C]TMSX was denoted as [^{11}C]KF18446.

times of that in the thalamus, and was 3.7 times of that in the frontal cortex. Our result demonstrated that the BP was smaller in the frontal lobe than in the temporal, occipital, and parietal lobes, although the postmortem study reported that the [^{3}H]SCH58261 binging in the frontal lobe was 1.5 times of those in the temporal and occipital lobes. Taken together these finding, imaging by [^{11}C]TMSX PET reflects distribution of adenosine A_{2A} receptors previously reported, although regional differences in the signals of specific binding of [^{11}C]TMSX were relatively small compared with those of other radioligands. The difference of results may be involved in methodology, such as species, tracer, autoradiography and anesthesia. To investigate the reason of the difference, further studies of living human brain will be needed using other PET ligand, such as [^{11}C]KF21213 (Wang et al., 2000) and [^{11}C]SCH44241 (Todde et al., 2000). Unfortunately, no data are available on the PET ligand for adenosine A_{2A} receptors in living human brain other than [^{11}C]TMSX (Ishiwata et al., 2005).

Past studies proved a functional interaction between adenosine A_{2A} and dopamine D_2 receptors (Fredholm and Svenningsson, 2003). Adenosine A_{2A} receptor is known to be concerned with not only modulation of dopamine, but also that of GABA and glutamate (Mori and Shindou, 2003; Popoli et al., 2003). Our human study showed that adenosine A_{2A} receptors are enriched in dopamine-rich areas, but that the receptors are also distributed in other regions as well as past studies. The adenosine A_{2A} receptors other than classical receptors modulating dopamine are called as "atypical adenosine A_{2A} receptor" (Ishiwata et al., 2000a; Lindstrom et al., 1996). The atypical adenosine A_{2A} receptors may be involved in the cerebral cortex, cerebellum, and thalamus.

In the study of [^{11}C]SCH44241 in monkey (Moresco et al., 2005), the BP was calculated using reference tissue model using the cerebellum as a reference region (Gunn et al., 1997). However, this article also showed that the binding of [^{11}C]SCH44241 was reduced by the administration of KW6002 not only in the striatum but also in the cortex and cerebellum. The result indicated the existence of the specific binding to adenosine A_{2A} receptor in the cerebellum, and the cerebellum is not an ideal reference region. Our data showed that specific binding was over 30% in the human cerebellum, cerebral cortex, and thalamus. In the human [^{11}C]TMSX PET, reference tissue model cannot be applied to calculation of BP with the region of interest (ROI) value of cerebellum, cerebral cortex and thalamus. The centrum semiovale is the region with lowest [^{11}C]TMSX binding, and was considered to be devoid of specific binding, because few neurons exist there. In our kinetic analysis, therefore, we used the ROIs over the centrum semiovale as a reference region (Naganawa et al., 2007).

In the animal study, percentage of unchanged [^{11}C]TMSX in plasma was 80.8% at 30 min in mice, and 41.7% at 30 min and 28.7% at 60 min in a monkey (Ishiwata et al., 2000a). To compare with the monkey, peripheral degradation of [^{11}C]TMSX was very slow in humans. The labeled metabolites may be negligible in the human [^{11}C]TMSX PET examination.

We are interested in human pathological condition of adenosine A_{2A} receptors, especially Parkinson's disease. As stated above, selective adenosine A_{2A} receptor antagonists are promising antiparkinsonian agents (Bara-Jimenez et al., 2003; Hauser et al., 2003). A postmortem study suggested that the density of adenosine A_{2A} receptors was increased in striatopallidal pathway neurons of Parkinson's disease with dyskinesias following long-term levodopa therapy (Calon et al., 2004). To date, clinical evidence is lacking about adenosine A_{2A} receptors of drug naive Parkinson's disease and its alteration after antiparkinsonian treatment. We expect that application of [^{11}C]TMSX PET will demonstrate the unknown mechanism of side effects of antiparkinsonian agents.

In conclusion, [^{11}C]TMSX PET demonstrated that adenosine A_{2A} receptors are enriched in the striatum, as well as postmortem and animal studies reported. However, the human distribution of the adenosine A_{2A} receptor is larger in the thalamus and cerebellum to compare with other mammals. To date, [^{11}C]TMSX is the only promising PET ligand, which is available to clinical use for mapping the adenosine A_{2A} receptors in the living human brain.

ACKNOWLEDGMENTS

The authors thank Dr. T. Oda for production of [^{11}C]TMSX; Ms. H. Tsukinari taking care of the subjects undergoing PET scanning.

REFERENCES

Ardekani BA, Braun M, Hutton BF, Kanno I, Iida H. 1995. A fully automatic multimodality image registration algorithm. J Comput Assist Tomogr 19(4):615–623.

Ascherio A, Zhang SM, Hernan MA, Kawachi I, Colditz GA, Speizer FE, Willett WC. 2001. Prospective study of caffeine consumption and risk of Parkinson's disease in men and women. Ann Neurol 50(1):56–63.

Bara-Jimenez W, Sherzai A, Dimitrova T, Favit A, Bibbiani F, Gillespie M, Morris MJ, Mouradian MM, Chase TN. 2003. Adenosine A_{2A} receptor antagonist treatment of Parkinson's disease. Neurology 61(3):293–296.

Calon F, Dridi M, Hornykiewicz O, Bedard PJ, Rajput AH, Di Paolo T. 2004. Increased adenosine A_{2A} receptors in the brain of Parkinson's disease patients with dyskinesias. Brain 127:1075–1084.

Dunwiddie TV, Masino SA. 2001. The role and regulation of adenosine in the central nervous system. Annu Rev Neurosci 24:31–55.

Ferre S, von Euler G, Johansson B, Fredholm BB, Fuxe K. 1991. Stimulation of high-affinity adenosine A_2 receptors decreases the affinity of dopamine D_2 receptors in rat striatal membranes. Proc Natl Acad Sci USA 88(16):7238–7241.

Fredholm BB, Svenningsson P. 2003. Adenosine-dopamine interactions: Development of a concept and some comments on therapeutic possibilities. Neurology 61(Suppl):S5–S9.

Fredholm BB, IJzerman AP, Jacobson KA, Klotz KN, Linden J. 2001. International Union of Pharmacology. XXV. Nomenclature and classification of adenosine receptors. Pharmacol Rev 53(4): 527–552.

Fujiwara T, Watanuki S, Yamamoto S, Miyake M, Seo S, Itoh M, Ishii K, Orihara H, Fukuda H, Satoh T, Kitamura K, Tanaka K, Takahashi S. 1997. Performance evaluation of a large axial field-of-view PET scanner: SET-2400W. Ann Nucl Med 11(4):307–313.

Fukumitsu N, Ishii K, Kimura Y, Oda K, Sasaki T, Mori Y, Ishiwata K. 2005. Adenosine A_1 receptor mapping of the human brain by PET with 8-dicyclopropylmethyl-1-^{11}C-methyl-3-propylxanthine. J Nucl Med 46(1):32–37.

Gunn RN, Lammertsma AA, Hume SP, Cunningham VJ. 1997. Parametric imaging of ligand-receptor binding in PET using a simplified reference region model. NeuroImage 6(4):279–287.

Hauser RA, Hubble JP, Truong DD. 2003. Randomized trial of the adenosine A_{2A} receptor antagonist istradefylline in advanced PD. Neurology 61(3):297–303.

Ishiwata K, Noguchi J, Toyama H, Sakiyama Y, Koike N, Ishii S, Oda K, Endo K, Suzuki F, Senda M. 1996. Synthesis and preliminary evaluation of [^{11}C]KF17837, a selective adenosine A_{2A} antagonist. Appl Radiat Isot 47(5/6):507–511.

Ishiwata K, Noguchi J, Wakabayashi S, Shimada J, Ogi N, Nariai T, Tanaka A, Endo K, Suzuki F, Senda M. 2000a. ^{11}C-labeled KF18446: A potential central nervous system adenosine A_{2A} receptor ligand. J Nucl Med 41(2):345–354.

Ishiwata K, Ogi N, Shimada J, Nonaka H, Tanaka A, Suzuki F, Senda M. 2000b. Further characterization of a CNS adenosine A_{2A} receptor ligand [^{11}C]KF18446 with in vitro autoradiography and in vivo tissue uptake. Ann Nucl Med 14(2):81–89.

Ishiwata K, Ogi N, Hayakawa N, Oda K, Nagaoka T, Toyama H, Suzuki F, Endo K, Tanaka A, Senda M. 2002. Adenosine A_{2A} receptor imaging with [^{11}C]KF18446 PET in the rat brain after quinolinic acid lesion: Comparison with the dopamine receptor imaging. Ann Nucl Med 16(7):467–475.

Ishiwata K, Wang WF, Kimura Y, Kawamura K, Ishii K. 2003. Preclinical studies on [^{11}C]TMSX for mapping adenosine A_{2A} receptors by positron emission tomography. Ann Nucl Med 17(3):205–211.

Ishiwata K, Mishina M, Kimura Y, Oda K, Sasaki T, Ishii K. 2005. First visualization of adenosine A_{2A} receptors in the human brain by positron emission tomography with [^{11}C]TMSX. Synapse 55(2): 133–136.

Kase H. 2001. New aspects of physiological and pathophysiological functions of adenosine A_{2A} receptor in basal ganglia. Biosci Biotechnol Biochem 65(7):1447–1457.

Kawamura K, Kimura Y, Tsukada H, Kobayashi T, Nishiyama S, Kakiuchi T, Ohba H, Harada N, Matsuno K, Ishii K, Ishiwata K. 2003. An increase of sigma receptors in the aged monkey brain. Neurobiol Aging 24(5):745–752.

Kimura Y, Ishii K, Fukumitsu N, Oda K, Sasaki T, Kawamura K, Ishiwata K. 2004. Quantitative analysis of adenosine A_1 receptors in human brain using positron emission tomography and [1-methyl-^{11}C]8-dicyclopropylmethyl-1-methyl-3-propylxanthine. Nucl Med Biol 31(8):975–981.

Kostic VS, Svetel M, Sternic N, Dragasevic N, Przedborski S. 1999. Theophylline increases "on" time in advanced parkinsonian patients. Neurology 52(9):1916.

Kulisevsky J, Barbanoj M, Gironell A, Antonijoan R, Casas M, Pascual-Sedano B. 2002. A double-blind crossover, placebo-controlled study of the adenosine A_{2A} antagonist theophylline in Parkinson's disease. Clin Neuropharmacol 25(1):25–31.

Latini S, Pedata F. 2001. Adenosine in the central nervous system: Release mechanisms and extracellular concentrations. J Neurochem 79(3):463–484.

Lindstrom K, Ongini E, Fredholm BB. 1996. The selective adenosine A_{2A} receptor antagonist SCH 58261 discriminates between two different binding sites for [^{3}H]-CGS 21680 in the rat brain. Naunyn Schmiedebergs Arch Pharmacol 354(4):539–541.

Logan J. 2003. A review of graphical methods for tracer studies and strategies to reduce bias. Nucl Med Biol 30(8):833–844.

Martinez-Mir MI, Probst A, Palacios JM. 1991. Adenosine A_2 receptors: Selective localization in the human basal ganglia and alterations with disease. Neuroscience 42(3):697–706.

Mishina M, Senda M, Kimura Y, Toyama H, Ishiwata K, Ohyama M, Nariai T, Ishii K, Oda K, Sasaki T, Kitamura S, Katayama Y. 2000. Intrasubject correlation between static scan and distribution volume images for [^{11}C]flumazenil PET. Ann Nucl Med 14(3):193–198.

Moresco RM, Todde S, Belloli S, Simonelli P, Panzacchi A, Rigamonti M, Galli-Kienle M, Fazio F. 2005. In vivo imaging of adenosine A_{2A} receptors in rat and primate brain using [^{11}C]SCH442416. Eur J Nucl Med Mol Imaging 32(4):405–413.

Mori A, Shindou T. 2003. Modulation of GABAergic transmission in the striatopallidal system by adenosine A_{2A} receptors: A potential mechanism for the antiparkinsonian effects of A_{2A} antagonists. Neurology 61(Suppl):S44–S48.

Naganawa M, Kimura Y, Mishina M, Manabe Y, Chihara K, Oda K, Ishii K, Ishiwata K. 2007. Quantification of adenosine A_{2A} receptors in the human brain using [^{11}C]TMSX and positron emission tomography. Eur J Nucl Med 34:679–687.

Popoli P, Frank C, Tebano MT, Potenza RL, Pintor A, Domenici MR, Nazzicone V, Pezzola A, Reggio R. 2003. Modulation of glutamate release and excitotoxicity by adenosine A2A receptors. Neurology 61(Suppl):S69–S71.